Integrated diesel production from lignocellulosic sugars via oleaginous yeast

Journal:	*Green Chemistry*
Manuscript ID	GC-ART-06-2018-001905.R1
Article Type:	Paper
Date Submitted by the Author:	23-Jul-2018
Complete List of Authors:	Sànchez i Nogué, Violeta; National Renewable Energy Laboratory, National Bioenergy Center Black, Brenna; National Renewable Energy Laboratory, National Bioenergy Center Kruger, Jacob; National Renewable Energy Laboratory, Singer, Christine; National Renewable Energy Laboratory, National Bioenergy Center Ramirez, Kelsey; National Renewable Energy Laboratory, National Bioenergy Center Reed, Michelle; National Renewable Energy Laboratory, Cleveland, Nicholas; National Renewable Energy Laboratory, National Bioenergy Center Singer, Emily; National Renewable Energy Laboratory, National Bioenergy Center Yi, Xiunan; National Renewable Energy Laboratory, National Bioenergy Center Yeap, Rou Yi; National Renewable Energy Laboratory, National Bioenergy Center Linger, Jeffrey; National Renewable Energy Laboratory, National Bioenergy Center Beckham, Gregg; National Renewable Energy Laboratory, National Bioenergy Center

Green Chemistry

PAPER

View Article Online
View Journal | View Issue

Integrated diesel production from lignocellulosic sugars via oleaginous yeast†

Violeta Sànchez i Nogué[1§], Brenna A. Black[2§], Jacob S. Kruger[1§], Christine A. Singer[1], Kelsey J. Ramirez[2], Michelle L. Reed[2], Nicholas S. Cleveland[1], Emily R. Singer[1], Xiunan Yi[1], Rou Yi Yeap[1], Jeffrey G. Linger[1], and Gregg T. Beckham[1,*]

Abstract: Oleaginous microbes are promising platform strains for the production of renewable diesel and fatty-acid derived chemicals given their innate capacity to produce high lipid yields from lignocellulose-derived sugars. Substantial efforts have been conducted to engineer model oleaginous yeasts primarily on model feedstocks, but to enable lipid production from biomass, judicious strain selection based on phenotypes beneficial for processing, performance on realistic feedstocks, and process integration aspects from sugars to fuels should be examined holistically. To that end, here we report the bench-scale production of diesel blendstock using a biological-catalytic hybrid process based on oleaginous yeast. This work includes flask screening of 31 oleaginous yeast strains, evaluated based on baseline lipid profiles and sugar consumption with corn stover hydrolysate. Three strains were down-selected for bioreactor performance evaluation. The cultivation results reveal that *Cryptococcus curvatus* ATCC 20509 and *Rhodosporodium toruloides* DSM-4444 exhibit equivalent fatty acid methyl ester (FAME) yield (0.24 g g^{-1}), whereas the highest overall FAME productivity (0.22 g L^{-1} h^{-1}) was obtained with *C. curvatus,* and *R. toruloides* displayed the highest final FAME titer (23.3 g L^{-1}). Time-resolved lipid profiling (including neutral and polar lipid classing) demonstrated triacylglycerol accumulation as the predominant lipid class in all strains. When evaluating tolerance mechanisms to inhibitory compounds, all strains can reduce and oxidize 5-(hydroxymethyl)furfural, illustrating parallel detoxification mechanisms. The *R. toruloides* strain is also capable of growth on four aromatic compounds as a sole carbon source, suggesting its use as a strain for simultaneous sugar and lignin conversion. Lipids from *R. toruloides* were recovered using a mild acid treatment and extraction, hydrogenated, and isomerized to produce a renewable diesel blendstock. The blendstock exhibited a cloud point of -14.5°C and simulated distillation showed that approximately 75% of the product was in the diesel range with a T90 consistent with No. 2 diesel fuel. Taken together, these results demonstrate an integrated process for renewable diesel production, identify oleaginous strains for further development, and highlight opportunities for improvements to an oleaginous microbial platform for the production of renewable diesel blendstock.

1. National Bioenergy Center, National Renewable Energy Laboratory, Golden CO 80401
2. Biosciences Center, National Renewable Energy Laboratory, Golden CO 80401 USA
§ Authors contributed equally to this work.
** gregg.beckham@nrel.gov*
† Electronic Supplementary Information (ESI) available: Materials and methods, strains used in this study, triacylglycerols and polar lipid speciation, sugar consumption profiles on mock hydrolysate, and growth profiles on aromatic compounds.

Introduction

The continued drive towards renewable transportation fuels will rely on lignocellulosic biomass as a primary feedstock.[1] Over the last several decades, a massive body of work has been conducted towards the development and deployment of lignocellulosic ethanol, especially accelerated in the last decade, and now pioneer plants are emerging, albeit slowly and not without serious technical challenges at the industrial scale.[2] Beyond ethanol production, there is a need for the production of a more comprehensive renewable fuels portfolio to satisfy the diesel, jet fuel, and gasoline markets. Many conversion pathways are being evaluated today to produce hydrocarbon fuels from lignocellulosic biomass. These pathways include multiple deconstruction technologies to produce biomass-derived sugars followed by biological, catalytic, or hybrid biological-catalytic approaches to upgrade sugars to fuel molecules.[3-9]

Biological routes to upgrade sugars directly to fuels beyond ethanol are quite varied. Peralta-Yahya *et al.* broadly categorized advanced biofuels directly available from biological routes according to their respective metabolic pathway as alcohol, fatty acid, isoprenoid, and polyketide-derived fuels.[10] Certainly other biologically derived

intermediates can be produced outside of this categorization that can then be catalytically converted to fuels, but the catalytic steps are usually more involved than simple hydrogenation or hydrodeoxygenation reactions (e.g., in the case of farnesene to farnesane).[11] To date, fuel precursors derived from fatty acid biosynthesis in particular have received significant attention, given that many microbes produce lipids in the C16-C20 range, which is an ideal carbon chain length for diesel. Fatty acids have to be either biologically or catalytically converted to esters, alcohols, or preferably branched alkanes before being used as diesel.[12-15]

For any given biotechnological application, microorganism selection will dictate the challenges faced during process development. In the case of lipid production as a diesel blendstock, selection among oleaginous microorganisms for strains with high flux would be highly beneficial, as they naturally accumulate a considerable fraction of their cell weight as lipids, and its composition is generally quite similar to that of common biodiesel feedstock. Moreover, the use of lignocellulosic biomass as a feedstock ideally demands for two additional crucial traits which will potentially accelerate the development to economic feasibility: i) the capability of the organism to simultaneously consume all present sugars, including hexoses and pentoses, and ii) a high tolerance to lignocellulosic-derived inhibitors present in the hydrolysates.[16] Given the growing interest in the production of diesel-range hydrocarbons from renewable feedstocks, many oleaginous microbes have been well studied in the last decade, including *Yarrowia lipolytica*,[17-20] *Cryptococcus curvatus*,[21, 22] *Rhodosporidium toruloides*,[23-27] *Rhodotorula glutinis* (the anamorph of *R. toruloides*),[28-30] and *Lipomyces starkeyi*[31-33] as they naturally possess several of these desired traits. Oleaginous microbes are typically not as genetically tractable as model bacteria and yeast, but metabolic engineering in *Y. lipolytica* has recently led to dramatic improvements in lipid titer, rate, and yield on clean sugars.[17, 20, 34, 35] Significant improvements in genetic engineering strategies to increase the expression of enzymes involved in different aspects of lipid biosynthesis has also been accomplished in *R. toruloides*.[36] As an alternative, many studies focusing on fatty acid-derived fuels have examined metabolic engineering strategies to increase production of fatty acids (mainly triacylglycerides) in model microorganisms such as *Saccharomyces cerevisiae* or *Escherichia coli*.[37-46] These studies have led to substantially higher lipid yields in these model organisms, but carbon flux is still quite limited relative to oleaginous microorganisms, which naturally accumulate lipids intracellularly as a stress response during nutrient deprivation.[47, 48]

Despite exciting advances in the production of microbial lipids, significant work remains to realize the potential of renewable diesel production, especially regarding process integration between the bioconversion step and the catalytic lipid conversion into diesel blendstock. Moreover, technoeconomic analyses have identified the need of product recovery due to intracellular accumulation, and the aerobic cultivation conditions during the bioconversion process among the primary cost drivers.[49, 50]

In this work, we report on bench-scale production of diesel blendstock using a biological-catalytic hybrid process by converting lignocellulosic-based sugars to lipid fuel precursors using the oleaginous yeast *R. toruloides* and upgrading them via a hydrotreating process (**Figure 1**). Specifically, we screened a total of 31 different oleaginous yeast strains on corn stover hydrolysate for lipid production capabilities. Three strains were selected and further characterized in terms of lipid profiling, including neutral and polar lipid classing, demonstrating the accumulation of neutral lipids, mainly triacylglycerols (TAGs), over the course of the cultivation on corn stover hydrolysate. Moreover, the detoxification capability of the selected oleaginous strains to inhibitory compounds present in lignocellulosic-based hydrolysate was evaluated using a mock hydrolysate, demonstrating their capability of reducing and oxidizing aldehydes, and converting aromatic compounds. Furthermore, *R. toruloides* DSM-4444 was the only strain capable of using four different aromatic compounds as a sole carbon source. Cells of *R. toruloides* DSM-4444 were employed in a cell lysis and extraction process to isolate the lipid fraction, which was subjected to catalytic conversion (consisting of hydrodeoxygenation (HDO) and hydroisomerization (HI)) leading to a product within the range for diesel fuel. To our knowledge, this is the first report describing an integrated process for the production of diesel blendstock from lignocellulosic-based sugars using a biological-catalytic hybrid process.

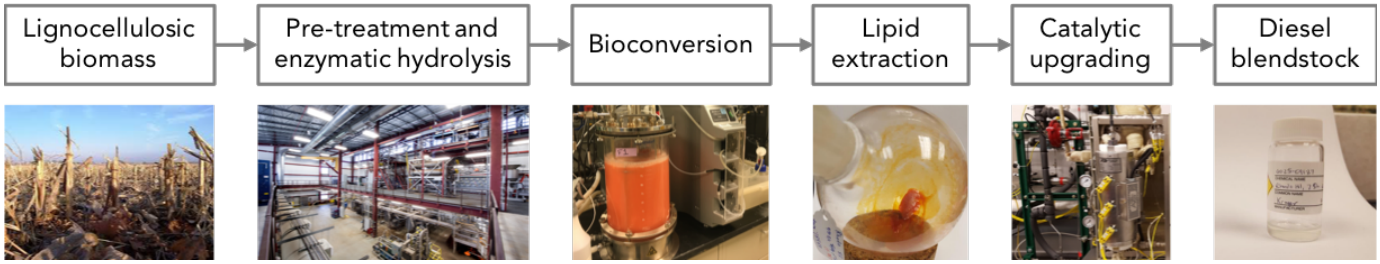

Figure 1. Process steps for the production of diesel blendstock from lignocellulosic biomass. In this work, bioconversion of lignocellulosic-based sugars to lipid fuel precursors is presented.

Results

Yeast screening on de-acetylated, dilute-acid pretreated, enzymatically hydrolyzed (DDAP-EH) corn stover hydrolysate

Small-scale strain screening is a useful strategy to evaluate a large number of strains in a systematic manner and to be able to quickly down-select the top performing candidates for a given application. However, the outcome of any screening procedure is highly dependent on the substrate of choice and cultivation conditions. This becomes especially critical when the final composition of the cultivation media triggers multiple synergistic effects regarding inhibition of metabolic events due to an increased pressure by compounds present in the growth medium. The importance of this was clearly exposed by Slininger *et al*.[51] in a screening to select good candidates for producing single cell oil from hydrolysates, when three of the top seven performing strains on synthetic medium reported by Dien and co-workers[52] did not grow on AFEX pretreated corn stover hydrolysate.[51, 52] Thus, in this study, the yeast screening to identify the strain with the best lipid production potential was performed using the same DDAP-EH corn stover hydrolysate to be used in the bioreactor evaluations. A total of 31 different yeast strains (listed in **Table S1**), belonging to seven different species, were screened in shake flasks on DDAP-EH corn stover hydrolysate diluted to an initial composition of 100 g L^{-1} monomeric sugars (glucose,

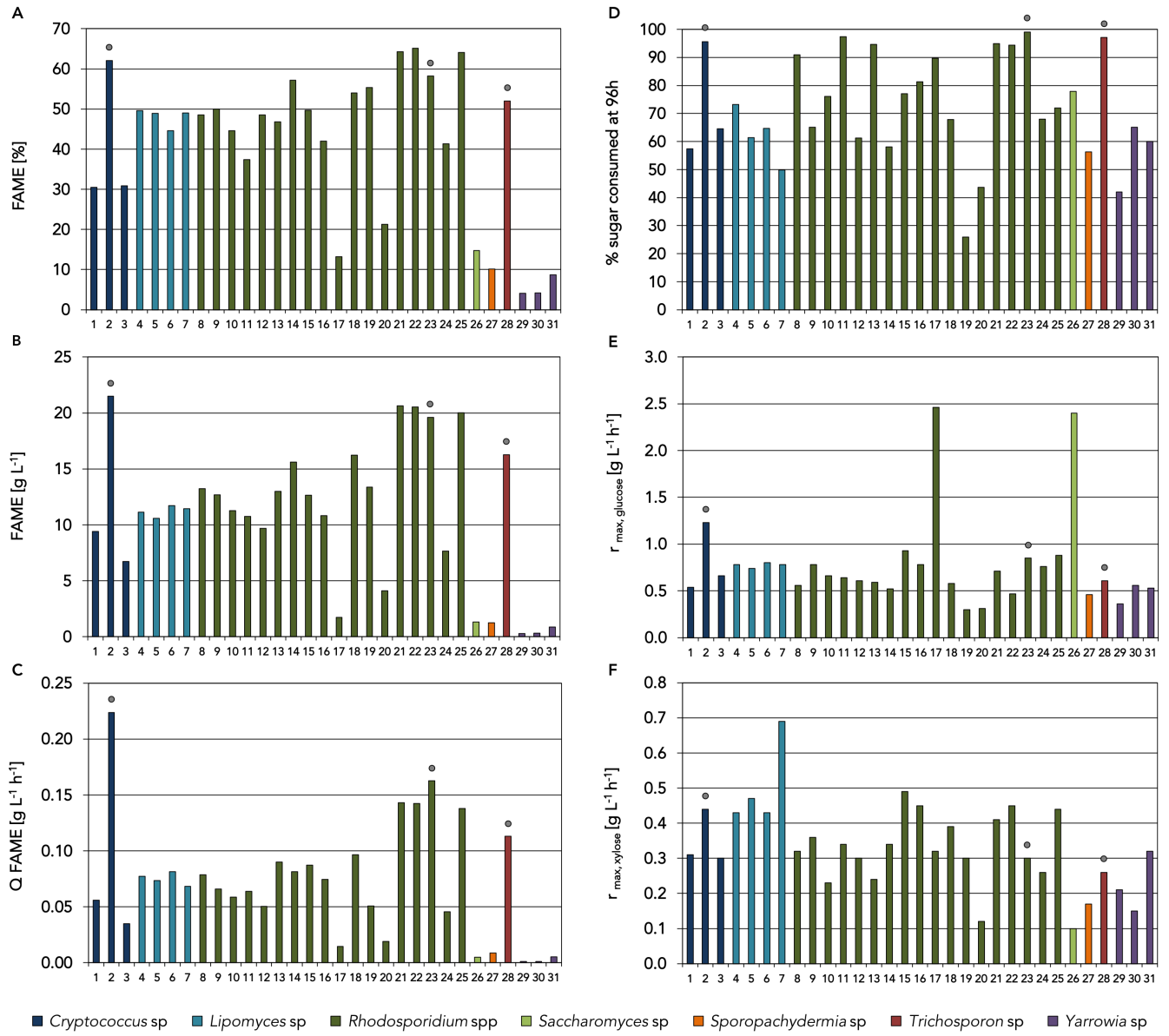

Figure 2. Lipid profiling measured as Fatty Acid Methyl Ester (FAME) determination, and sugar consumption from shake flask yeast screening on DDAP-EH corn stover hydrolysate. FAME content (%)(A), FAME titer (B), and FAME productivity (Q) (C), total sugar consumed at 96 h of cultivation (D), maximum glucose (E), xylose (F) consumption rates ($r_{max, sugar}$). The selected strains for further evaluation are highlighted with the symbol ●.

xylose, arabinose, and galactose) and supplemented with growth factors (yeast extract and peptone) (**Figure 2**).

Over the course of this study, some yeast species names have been updated based on ribosomal sequencing[53] and revisions on taxonomy (Dr. Kyria Boundy-Mills, personal communication). Since not all yeast culture collections have undergone a taxonomical revision, old species names have been maintained throughout the main text for clarity, and the updated names are included in **Table S1**.

All strains were inoculated at an optical density at 600 nm (OD_{600}) of 1.0 and monitored for growth and sugar consumption. Upon sugar depletion, a yeast biomass sample was taken, lyophilized, and its baseline lipid profiling was measured as fatty acid methyl ester (FAME). Candidate strains to be evaluated in fully controlled bioreactors were down-selected considering first FAME parameters, and then sugar consumption (**Figure 2**). To capture consumption of multiple sugars, the percentage of utilized sugars after 96 hours of cultivation was chosen as the criterion to compare the strains, as glucose and xylose depletion was observed for all strains between 72 and 192, and 120 and 216 hours of cultivation, respectively (data not shown). The strain *Cryptococcus curvatus* ATCC 20509 (strain #2 in **Figure 2**) consistently displayed the highest values, with a 62.12 % of FAME content (**Figure 2A**), up to 21.49 g L^{-1} final FAME titer (**Figure 2B**), and a FAME productivity of 0.22 g L^{-1} h^{-1} (**Figure 2C**). Thus, it was selected for further evaluation in fully controlled bioreactors. Among all tested *Rhodosporidium* strains included in this screening, four different *R. toruloides* strains (Y-27012, Y-27013, DSM-4444, and DSM-70398 – strains #21, #22, #23, and #25, respectively in **Figure 2)** were the best performers. Since they displayed similar values of FAME parameters, sugar consumption was also taken into consideration to down-select among those *R. toruloides* strains. After 96 h of cultivation, up to 99% of total sugars were consumed by the DSM-4444 strain, whereas less than 95% was consumed by the Y-27012 and Y-27013 strains. In the case of the DSM-70398 strain, less than 72% of total sugar was consumed after 96 h of cultivation (**Figure 2D**). Given the differences in sugar consumption rates, the DSM-4444 strain was selected as the candidate among the *Rhodosporidium* strains tested. In addition, *Trichosporon guehoae* UCDFST 60-59 strain (strain #28 in **Figure 2**) was also selected to be further evaluated in fully controlled bioreactors. This strain displayed a lower level of FAME content (51.97%) compared to the selected *C. curvatus* and *R. toruloides* strains, but similar to the *Lipomyces starkeyi* strains included in this screening (strains from #4 to #7 in **Figure 2A**). The UCDFST 60-59 strain was selected over *Lipomyces* strains, due to higher values of FAME titer (**Figure 2B**), FAME productivity (**Figure 2C**), and total sugar consumption after 96 h of cultivation relative to *Lipomyces* strains (**Figure 2D**). Regarding sugar consumption, most of the strains included in the screening displayed a maximum glucose consumption rate between 0.5 and 1 g L^{-1} h^{-1}, and only 3 strains exhibit values higher than 1 g L^{-1} h^{-1}: *C. curvatus* ATCC 20509 (1.23 g L^{-1} h^{-1}), *R. sphaerocarpum* UCDFST 68-43 (2.46 g L^{-1} h^{-1}), and the *Saccharomyces cerevisiae* strain D5A (2.40 g L^{-1} h^{-1}) (strains #2, #17, and #26, respectively in **Figure 2E**). Regarding maximum xylose consumption rate, all tested strains exhibit values below 0.5 g L^{-1} h^{-1}, except *L. starkeyi* UCSFST 78-23, which displayed the highest maximum xylose consumption rate of nearly 0.7 g L^{-1} h^{-1} (strain #7 in **Figure 2F**).

Selection of promising strains is highly dependent on the initial candidate strains under evaluation and the experimental conditions, especially when different lignocellulosic hydrolysates are used. Thus, comparison of screening processes in reported literature is quite challenging. For example, Slininger and coworkers evaluated 38 strains in the sequential screening on AFEX corn stover hydrolysate, and AFEX switchgrass hydrolysate using 96-well plates. The top performing strains, which were further evaluated in shake flask cultures using a two-stage lipid production strategy, were a *R. toruloides* strain and two *Lipomyces sp.* strains.[51] In the present work, *R. toruloides* strains were also identified as top candidates, but the tested *Lipomyces* strains were not ranked as the top performing strains because of low FAME accumulation, and thus not considered for further evaluation in fully controlled bioreactors. Instead, a *C. curvatus* strain and a *T. guehoae* strain were identified as top candidates. This example also clearly illustrates the importance of defining the screening conditions as analogous as possible to the application conditions, especially when complex substrates such as lignocellulosic-based feedstocks are being utilized.

Bioreactor cultivations on DDAP-EH

As shake flask screenings represent a fast and simple approach to obtain essential information, the larger, homogeneous volume when using a fully controlled bioreactor enables a more complete lipid analysis in a time-course fashion. Cultivations using the three strains selected for further evaluation (*C. curvatus* ATCC 20509, *R. toruloides* DSM-4444, and *T. guehoae* UCDFST 60-59) were thus performed in a 0.5 L controlled bioreactor on DDAPH-EH corn stover hydrolysate diluted to an initial composition of 100 g L^{-1} monomeric sugars (glucose, xylose, arabinose, and galactose) (**Table 1**). Seed cultures propagated for 24 hours on Yeast Nitrogen Base (YNB) medium supplemented with 50 g L^{-1} glucose and N-rich media components were used to inoculate the bioreactors at an OD_{600} of 1.0. In addition to growth and sugar consumption monitoring, cultures were sampled every 24 hours for FAME, free fatty acids, neutral lipids, and polar lipids analysis.

Table 1. Initial monomeric sugar concentrations in DDAP-EH corn stover hydrolysate and mock hydrolysate used in this study

Concentration	Glucose	Xylose	Arabinose	Galactose
g L^{-1}	58.17	34.63	5.11	2.09

C. curvatus ATCC 20509 displayed a sequential sugar consumption pattern where glucose was fully consumed

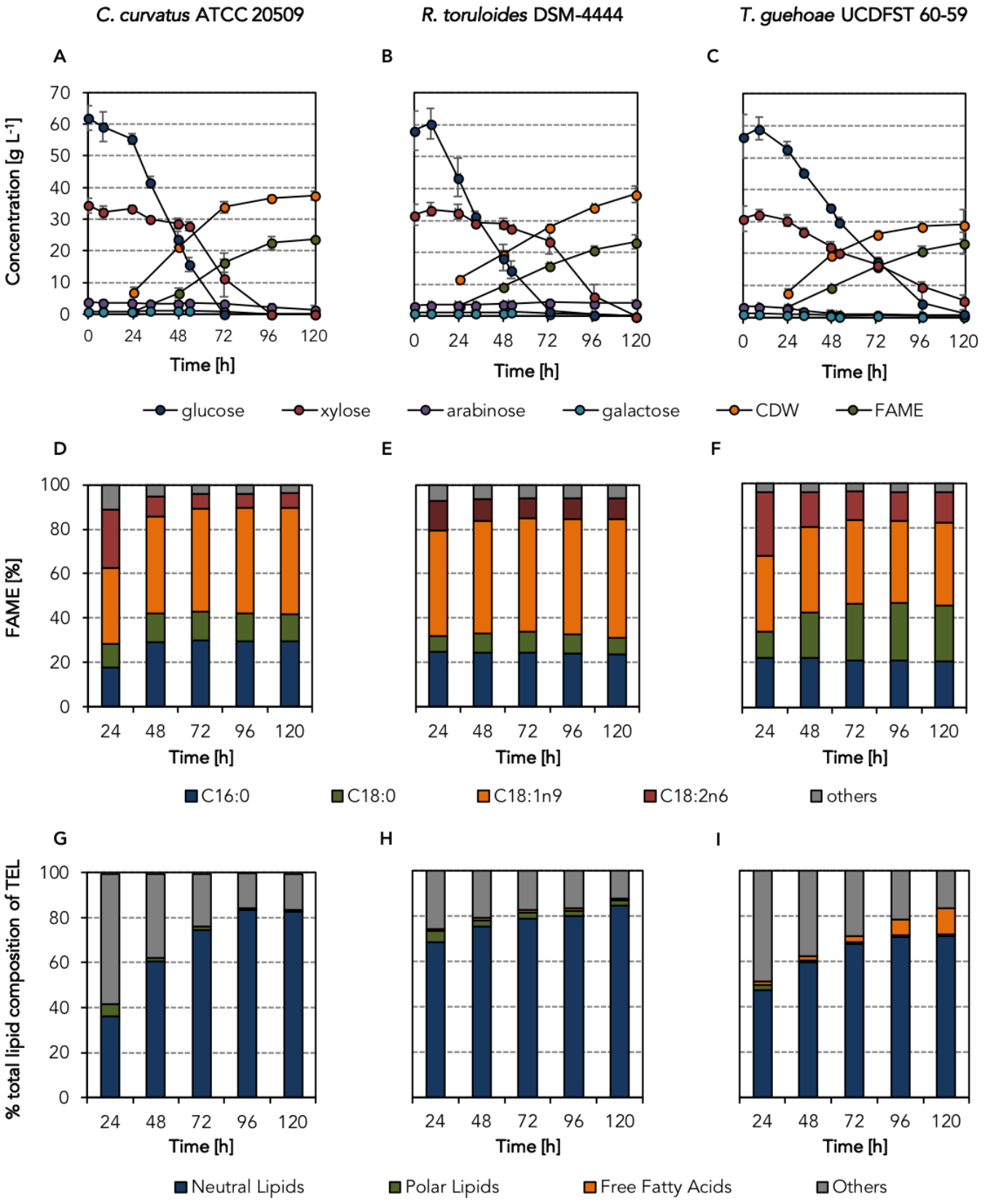

Figure 3. Bioreactor cultivations on DDAP-EH corn stover hydrolysate for *C. curvatus* ATCC 20509 (left column), *R. toruloides* DSM-4444 (middle column), and *T. guehoae* UCDFST 60-59 (right column) strains. Cultivation performance (A-C), FAME profiling (D-F), total lipid composition of total extractable lipids (G-I). Abbreviations: CDW: cell dry weight, FAME: fatty acid methyl ester, TEL: total extractable lipids

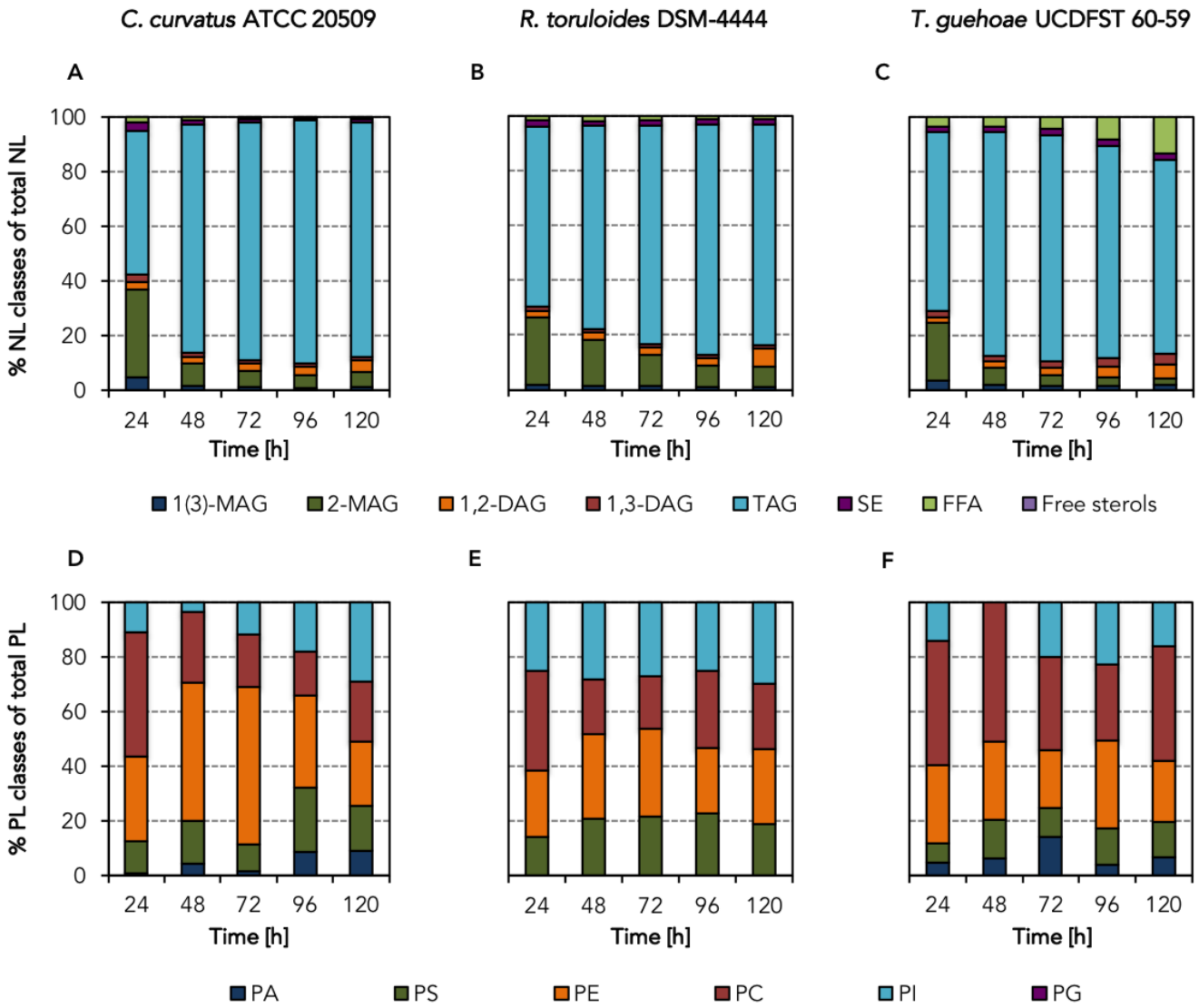

Figure 4. Bioreactor cultivations on DDAP-EH corn stover hydrolysate for *C. curvatus* ATCC 20509 (left column), *R. toruloides* DSM-4444 (middle column), and *T. guehoae* UCDFST 60-59 (right column) strains. Neutral lipids classing (A-C), and polar lipids classing (D-F). Abbreviations: NL: neutral lipids, PL: polar lipids, MAG: monoacylglycerol, DAG: diacylglycerol, TAG: triacylglycerol, SE: steryl ester, FFA: free fatty acid, PA: phosphatidic acid, PS: phosphatidylserine, PE: phosphatidylethanolamine, PC: phosphatidylcholine, PI: phosphatidylinositol, and PG: phosphatidylglycerol.

within 72 h, and clear xylose consumption was only observed when glucose levels were below 20 g L^{-1}. At the end of the cultivation, the FAME content of the *C. curvatus* strain was 63.1%, and up to 21.4 g L^{-1} FAME was obtained, representing a FAME yield of 0.24 g g^{-1} consumed sugars and overall FAME productivity of 0.22 g L^{-1} h^{-1} (**Figure 3A, Table 2**). Also, sequential sugar consumption was observed with *R. toruloides* DSM-4444. In this case, however, the glucose and xylose consumption rate were slower compared to the *C. curvatus* strain. As a consequence, the arabinose present in the cultivation media was not consumed after 120 h of cultivations. At the end of the cultivation, a slightly lower overall FAME productivity, and FAME content, 0.17 g L^{-1} h^{-1} and 60.8%, respectively, were observed. The final obtained FAME titer was 23.3 g L^{-1}, representing a FAME yield of 0.24 g g^{-1} consumed sugars (**Figure 3B, Table 2**). Differences in terms of sugar consumption were observed with the *T. guehoae* UCDFST 60-59 strain, where glucose and xylose, in addition to the minor sugars arabinose and galactose were co-consumed. Despite this pattern, glucose and xylose were not depleted after 120 h of cultivation, as all sugar consumption rates were slower than the ones observed with the *C. curvatus* and *R. toruloides* strains. At the end of the cultivation, a final FAME titer of 14.2 g L^{-1} was obtained, representing a FAME yield of 0.16 g g^{-1} consumed sugars. A significantly lower overall FAME productivity, 0.12 g L^{-1} h^{-1}, was obtained with *T. guehoae* compared to *C. curvatus*. Also, the final FAME content was significantly lower, 48.3 %, compared to that obtained with the other strains (**Figure 3C, Table 2**).

The strain *C. curvatus* ATCC 20509 has previously been evaluated on other lignocellulosic-based feedstocks. A higher yield was obtained but a lower lipid content was

Table 2. Cultivation performance parameters on DDAP-EH corn stover hydrolysate

Strain	% FAME	FAME [g L^{-1}]	Q FAME [g L^{-1} h^{-1}]	Y FAME [g g^{-1}]	Y biomass [g g^{-1}]
C. curvatus ATCC 20509	63.1 ± 3.7	21.4 ± 3.6	0.22 ± 0.03	0.24 ± 0.03	0.37 ± 0.03
R. toruloides DSM-4444	60.8 ± 1.1	23.3 ± 1.8	0.17 ± 0.04	0.24 ± 0.05	0.39 ± 0.08
T. guehoae UCDFST 60-59	48.3 ± 4.0	14.2 ± 3.3	0.12 ± 0.03	0.16 ± 0.05	0.33 ± 0.08

achieved when the performance of this strain was evaluated on sorghum stalk (0.29 g g^{-1} sugar and 60%, respectively) and switchgrass hydrolysate (0.27 g g^{-1} sugar and 58%, respectively) compared to the results obtained in the present study.[54] A much lower lipid performance was obtained with this strain when using dilute acid pretreated wheat straw hydrolysate. In this case, a lower FAME productivity (0.03 g L^{-1} h^{-1}), also coupled to a lower FAME content (33.5%) and yield (0.17 g g^{-1} sugar), demonstrating the presence of a higher level of inhibitors in this substrate.[55] Other *Cryptococcus* species have been also tested in other lignocellulosic-based feedstocks, such as corncob hydrolysates. In this case, and although a similar lipid content was obtained, much lower productivities and final titers were achieved, even when using fed-batch strategies.[56, 57] Overall, the results obtained with the *C. curvatus* strain on DDAP-EH corn stover hydrolysate positions the performance reported in this work among the best reported on lignocellulosic feedstocks. In the case of *R. toruloides*, different feeding strategies have been reported to improve the cultivation performance. The strain DSM-4444 was tested using the C6 fraction of corn stover hydrolysate, and compared to batch conditions, an increase of 43% in FAME productivity and 53% in yield was reported when the residual level of glucose was maintained at 10 g L^{-1} over the course of the cultivation.[58] The best performance to date on lignocellulosic-based hydrolysates has been reported with the *R. toruloides* Y4 strain, where up to 39.6 g L^{-1} of lipid titer and a productivity of 0.33 g L^{-1} h^{-1} was achieved under fed-batch conditions using concentrated Jerusalem artichoke hydrolysate.[59] Other oleaginous yeast have been tested on toxic hydrolysates or challenging conditions. For example, *L. starkeyi* performance was evaluated on thermochemical pretreated birch hydrolysate using a pH regulated fed-batch cultivation. In this case, acetic acid was co-consumed with xylose, and a final lipid titer of 8 g L^{-1} (representing a lipid yield of 0.1 g g^{-1}) coupled with a 51.3% lipid content was obtained.[60] Up to 5.78 g L^{-1} FAME were obtained when *Trichosporon cutaneum* was evaluated on corn stover at 20% solids.[61] Taken together, the obtained bioreactor results confirm that the screening conditions were optimal to identify the best lipid producing strains, as the results obtained for the three strains during the screening on shake flasks correlate well with the results obtained using fully controlled bioreactors.

Daily sampling, including yeast biomass, enabled FAME determination over the course of the bioreactor cultivations. FAME profiles for the three evaluated strains consisted essentially of the saturated palmitic (C16:0) and stearic (C18:0) acids, and the unsaturated oleic (C18:1n9) and linoleic (C18:2n6) acids. In the case of the *C. curvatus* cultivation, where the main fatty acids were palmitic and oleic acid, an increase of palmitic acid between 24 and 48 hours was observed, and the same level was maintained during the remainder of the cultivation. For the C18 fatty acids, a tendency to gain saturation over time was detected by decreasing levels of linoleic over oleic acid (**Figure 3D**). The FAME profiles in the case of the *R. toruloides* were more stable over time than in the two other evaluated strains. In this case, however, the highest fraction corresponded to oleic acid, at the expense of palmitic and stearic acid content (**Figure 3E**). In the *T. guehoae* cultivation, palmitic acid levels remained at the same levels over the course of the cultivation. Also, similarly to the *C. curvatus* strain, *T. guehoae* tended to gain saturation over time for the C18 fatty acids, where stearic and oleic acid content increased, and linoleic acid decreased between the 24 and 48 hours sampling point (**Figure 3F**). The presence of unsaturated linoleic acid in the FAME profile of all three oleaginous strains suggests the participation of at least two independent desaturase enzymes (Δ-9 fatty acid desaturase and Δ-12). Corresponding to the linoleic acid content in *C. curvatus* and *T. guehoae,* both Δ-9 and Δ-12 desaturase appeared to be more active in early exponential growth, and towards stationary phase of *T. guehoae* Δ-9 desaturase activity dropped resulting in less oleic and more saturated species. An increase in saturation of lipids with culture age has been previously observed in *Y. lipolytica* and other microorganisms.[62, 63]

In addition to the FAME profiles, total lipid composition (as a percentage of the total extractable lipids) was also analyzed over the course of the yeast cultivations. Since acid catalyzed FAME can be produced from the acyl chains of neutral lipids, polar lipids, and free fatty acids, it is important to understand the lipid source, not only because the backbone carbon waste from each lipid class is not equivalent, but heteroatoms such as phosphorus from the polar lipid class can be toxic to chemical catalysts. In the case of *C. curvatus*, free fatty acid levels remained minimal and stable over time, whereas neutral lipids increased during 96 h of cultivation and plateaued in the last sampling time point (120 h). An inverse tendency was observed in the case of polar lipids, with levels reduced after 48 h and remaining constant for the subsequent duration of the cultivation (**Figure 3G**). In the case of the *R. toruloides* strain, the

neutral lipid fraction increased monotonically over the course of the cultivation, but the overall increment was relatively lower, since the initial time point had a higher content than the other evaluated strains. Similar to *C. curvatus*, polar lipid levels of *R. toruloides* were reduced after 48 h, and remained at similar levels for the rest of the cultivation. Also, in this case, free fatty acid levels remained minimal and stable over time (**Figure 3H**). Additionally, like *C. curvatus*, the content of neutral lipids in the *T. guehoae* strain increased monotonically during the first 96 h of cultivation, and then plateaued in the last sampling time point (120 h), whereas the polar lipid fraction remained relatively stable over time. The main difference between *T. guehoae* and the other tested strains is the presence of a higher fraction of free fatty acids, which increased over the course of the cultivation (**Figure 3I**). This initial relative increase in polar lipid concentration in all strains likely accounts for the role that phosphatidic acid (PA) has on both neutral and polar lipid biosynthesis in the exponential growth phase wherein polar lipid synthesis is activated to contribute to cell membrane phospholipids. Simultaneously, PA also acts as an acyl-donor at this growth phase to assist in the formation of TAG. However, similarly with other oleaginous yeasts,[64] TAG synthesis increases through a neutral lipid pathway, thus increasing total neutral lipids over the cultivation time. Finally, the accumulation of free fatty acids of the *T. guehoae* strain over the harvest time indicates increased lipase activity of the organism compared to *C. curvatus* and *R. toruloides*.

Neutral and polar lipid classing was also performed in a time-resolved fashion. The *C. curvatus* strain displayed increasing levels of TAG over time between 24 and 48 hours and remained at more stable levels over time as the main neutral lipid class. This was coupled to a net decrease level of monoacylglycerols (1(3)-MAG, and 2-MAG), whereas the diacylglycerols (1,2-DAG and 1,3-DAG) levels remained essentially stable. Steryl ester and free fatty acid levels remained minimal and stable over the course of the cultivation (**Figure 4A**). In the case of the *R. toruloides* strain, TAG was also the main neutral lipid class, which increased over the first 72 h and maintained these levels until the end of the cultivation. This was combined with decreasing levels of 2-MAG over time, which plateaued in the last sampling point (120 h), whereas 1(3)-MAG and diacylglycerol levels remained stable over the course of the cultivation. Similarly to *C. curvatus*, steryl ester and free fatty acid levels remained minimal and stable over time for the *R. toruloides* strain (**Figure 4B**). The presence and subsequent decrease of MAG with the accumulation of TAG over the harvest time suggests the incorporation of MAG, either directly or indirectly, to TAG. To date, acyl-CoA:monoacylgycerol acyltransferases have not been described for yeast, although this re-esterification of MAG to DAG is an important step in plant and mammalian lipid metabolism.[65] MAG species comprising the neutral lipid pathway for TAG accumulation in these yeast strains warrants future study. As observed with the other two strains, TAG was also the main neutral lipid class in the *T. guehoae* strain cultivation. In addition, a similar trend as for the *C. curvatus* strain was observed, where increasing TAG levels were observed between 24 and 48 hours and remained at more stable levels during the course of the cultivation. This was coupled to an inverse trend of MAG levels. In addition, and a slight increase of DAG levels were observed over time. Similarly, with the other two strains, steryl ester levels remained minimal and stable over time, but contrary to the other strains, the *T. guehoae* strain clearly exhibits an increase of free fatty acid levels over the course of the cultivation (**Figure 4C**). The decrease in TAG with a corresponding increase in DAG and free fatty acids, indicates breakdown of TAG into its components and further strengthens the hypothesis of increased lipase activity towards the 120 h time point. Of the neutral lipid classing, TAG was further speciated to offer insight above that of FAME profiling (as shown in **Figure S2**).

Regarding polar lipid classing, phosphatidylethanolamine (PE) and phosphatidylcholine (PC) were initially the main classes observed in the *C. curvatus* strain. The initial levels of PC decreased at 48 h and remained stable over time, and the level of PE peaked at the 72 hours sampling point. This was coupled to an increase of phosphatidylinositol (PI) levels at the end of the cultivation, and a relatively stable level of PA (**Figure 4D**). Along with the absence of phosphatidylglycerol (PG), these observations follow the cytidine diphosphate diacylglcerol (CDP-DAG) pathway for yeast, where PA is converted to either PI or phosphatidylserine (PS), PS continues to be converted to PE, and finally to PC.[64, 66] With this in mind, the *C. curvatus* strain initially partitioned the CDP-DAG pathway towards PC, but towards the end point of the cultivation, PI additionally accumulates as well. For *R. toruloides*, there was only the presence of four different polar lipid classes (PE, PS, PI, and PC) at roughly similar levels, which remained stable over the course of the cultivation indicating that PA was being utilized rapidly (**Figure 4E**). Similarly to *R. toruloides*, levels of PA, PE, PS, PI, and PC remained relatively stable over the course of cultivation with the *T. guehoae* strain (**Figure 4F**). Similarly to TAG, polar lipid classes were also speciated, as reported in **Figure S3.**

The top three yeast strains selected for further evaluation exhibit similar lipid growth profiles. A thorough characterization of lipid production and sugar utilization over the course of cultivation shows that at 96 h, the majority of sugars were consumed for all three strains and lipid profiles were mature and did not alter with additional fermentation time (FAME, neutral, polar lipids), with the exception of lipase activity from *T. guehoae*. In addition to FAME profiling, lipid class profiling was necessary to determine fatty acid origin, and therefore, to ensure carbon to fuel precursor efficiency. Based on ideal fuel precursor (lipid class and fatty acid profile), as well as production parameters (yield, productivity, and titer), the optimal strains for further conversion would be *R. toruloides* and *C. curvatus*.

Cultivations on mock hydrolysate

When lignocellulosic biomass is hydrolyzed to release monomeric sugars, degradation compounds are also

formed. Aldehydes, such as 5-(hydroxymethyl)furfural (5-HMF) and furfural, are generated via sugar dehydration. In addition, aromatic compounds are released as result of lignin degradation. The presence of these compounds in the resulting hydrolysate can negatively impact the metabolism of microorganisms. To evaluate potential toxicity tolerance mechanisms, the selected strains were inoculated into a synthetic hydrolysate containing 100 g L^{-1} of total initial sugars (at the same ratio of glucose, xylose, arabinose, and galactose present in DDAP-EH corn stover hydrolysate) (**Table 1**), in addition to 8 different inhibitory compounds (5-HMF, 4-hydroxybenzaldehyde, vanillic acid, caffeic acid, syringic acid, vanillin, *p*-coumaric acid, and ferulic acid).

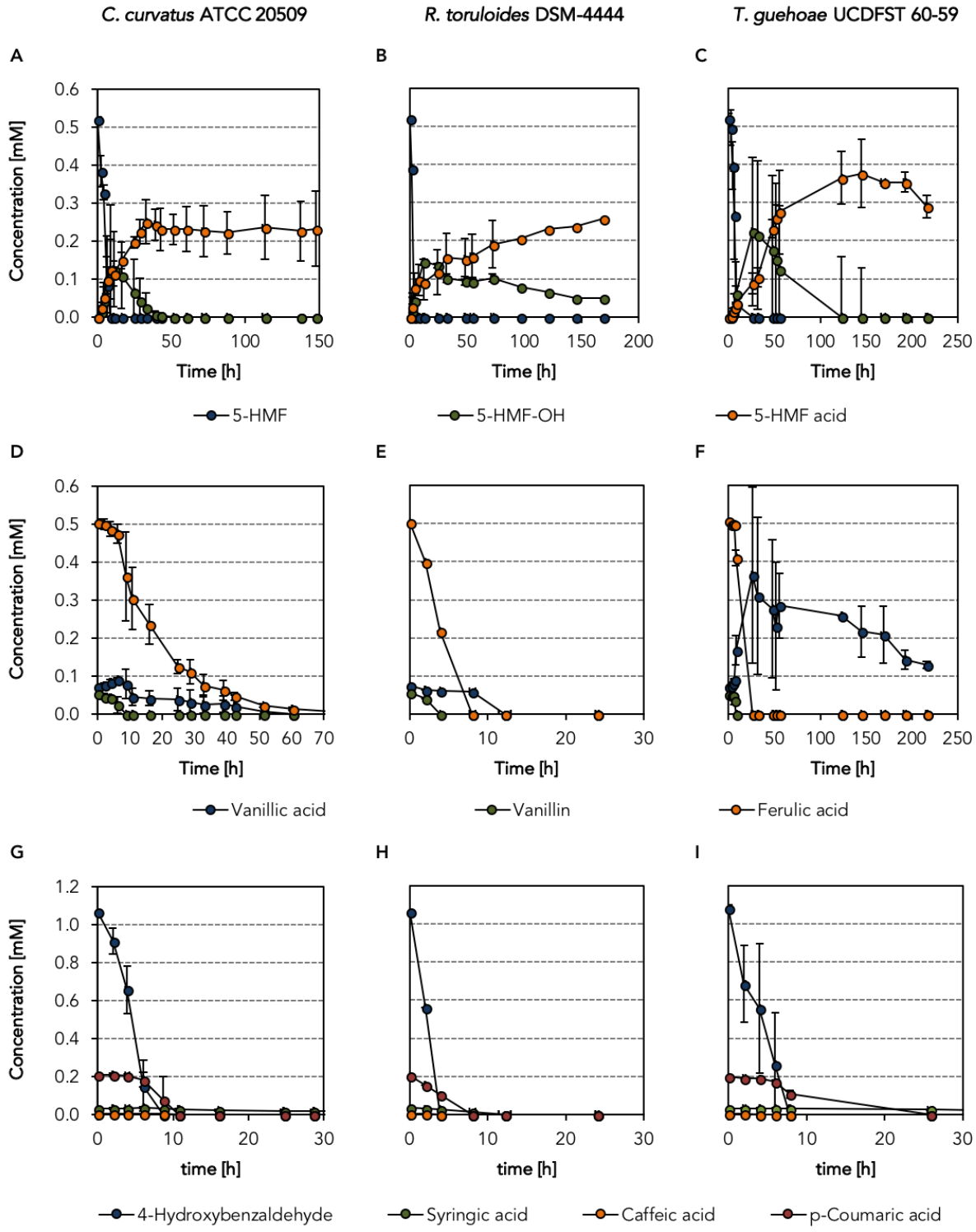

Figure 5. Shake flask cultivations on mock hydrolysate for *C. curvatus* ATCC 20509 (left column), *R. toruloides* DSM-4444 (middle column), and *T. guehoae* UCDFST 60-59 (right column) strains. For clarity, profiles of lignocellulosic degradation compounds are presented in different graphs.

To extend the conversion time profiles and asses conversion, concentrations of inhibitory compounds were doubled based of the ones present in DDAP-EH corn stover hydrolysate.

Strains were inoculated at the same OD_{600} of 1.0, and samples were taken over time for sugar assimilation and inhibitory compound conversion until the sugars were depleted (sugar profiles are summarized in **Figure S4**). In the case of the *C. curvatus* strain, 5-HMF was completely converted within 9 hours of cultivation. Although 5-HMF was simultaneously converted to 5-(hydroxymethyl)furfural alcohol (5-HMF alcohol) and 5-(hydroxymethyl)furfural acid (5-HMF acid), different trends where observed for these two compounds when 5-HMF was fully depleted. Specifically, the maximum 5-HMF alcohol concentration was observed when 5-HMF was fully depleted, and the 5-HMF acid level continued increasing due to a molar conversion of 5-HMF alcohol to 5-HMF acid. The level of 5-HMF acid remained stable for the rest of the cultivation (**Figure 5A**). Like 5-HMF, vanillin was also assimilated within 8 hours of cultivation. In the case of the aromatic acids, vanillic acid and ferulic acid were completely depleted after 60 and 87 hours of cultivation, respectively (**Figure 5D**). Similarly, decreasing profiles were observed for all the other inhibitors. Namely, 4-hydroxybenzaldehyde, caffeic, and *p*-coumaric acid were converted within the first 16 hours of cultivation, and up to 133 hours were required to have full conversion of syringic acid in the *C. curvatus* strain cultivation (**Figure 5G**).

Some important differences were observed with the *R. toruloides* strain. Initially, 5-HMF was also converted simultaneously to 5-HMF alcohol and 5-HMF acid within the first 4 hours of cultivation. Further conversion of 5-HMF alcohol to 5-HMF acid was slower than in *C. curvatus*, as 5-HMF alcohol was still detected when sugars were fully depleted (**Figure 5B**).

Overall, the *R. toruloides* strain showed a higher capability of inhibitor conversion, as all other degradation compounds initially present in mock hydrolysate were completely converted within 12 hours of cultivation (**Figure 5E and H**). In the case of *T. guehoae*, 5-HMF was also simultaneously converted to 5-HMF alcohol and 5-HMF acid, in this case within 24 hours of cultivation. Similarly to the *C. curvatus* strain cultivation, 5-HMF alcohol was completely depleted when sugars were still present in the media (**Figure 5C**). In addition, a unique catabolic pathway was observed for this strain, as ferulic acid was converted first to vanillic acid within 24 hours, and then re-assimilated over the course of the cultivation (**Figure 5F**). Conversion of ferulic acid to vanillic acid through the β-oxidation pathway has been extensively reported in bacteria, including among them, the oleaginous bacteria *Rhodocous opacus*.[67] In the case of fungal systems, this conversion is described via propenoic chain degradation instead,[68] and to the best of our knowledge the conversion of ferulic to vanillic acid is first shown for the oleaginous yeast *T. guehoae* in the present study. The accumulation of vanillic acid, however, would indicate a low efficiency on further assimilation. On the other hand, *p*-coumaric acid was also fully converted within 24 hours, and it required up to 8 hours in the case of 4-hydroxybenzaldehyde. Caffeic acid was assimilated within 6 hours, whereas it required up to 169 hours of cultivation in the case of syringic acid (**Figure 5I**).

Due to similar chemical structures, detoxification mechanisms and assimilation pathways for 5-HMF and furfural are often equivalent, and previously reported evidence can help to elucidate the different assimilation pathways in other microorganisms. Exclusive conversion of furfural to 2-furoic acid, not to furfuryl alcohol, has been observed in the case of *P. putida* and *E. coli,*[69] whereas the degradation of 5-HMF via HMF acid and its further metabolism through the furfural assimilation route has been described in the bacterium *Cupriavidus basilensis.*[70] Similarly to what was observed for 5-HMF with all the evaluated strains, simultaneous conversion of 5-HMF and furfural to its corresponding acids and alcohols has been also observed with the fungi *Amorphotheca resinae* ZN1[71] and *Pleurotus ostreatus.*[72] In the case of *T. fermentans*, another oleaginous yeast, this organism initially reduces furfural to furfuryl alcohol during the lag phase, and then the concentration of furfuryl alcohol decreases while the concentration of furoic acid increases,[73] as observed here with all tested strains. This capability to reduce and oxidize furanic compounds under aerobic conditions would suggest a versatility of detoxification mechanisms, contrary to *S. cerevisiae*, in which furfural was reported to be exclusively converted to furoic acid during respiratory growth, and to furfuryl alcohol during anaerobic growth.[74] Similarly to *Pleurotus ostreatus,*[72] *Cupriavidus basilensis,*[75] and an engineered *P. putida* strain,[76] the tested strains showed the potential ability to assimilate furaldehyde compounds to enhance carbon conversion of lignocellulosic streams.

Cultivations on mineral medium with aromatic compounds as carbon source

Valorization of lignin-rich streams in a biorefinery will be essential for the overall economic viability of lignocellulose conversion.[50] To assess if oleaginous yeasts could potentially be used as organisms for microbial lignin valorization strategies,[77] ferulic acid, vanillic acid, *p*-coumaric acid, and 4-hydroxybenzoic acid were tested as a sole carbon source. They have previously been identified in the lignin-enriched streams obtained from corn stover subjected to an alkaline pretreatment, and are often used as model aromatic lignin compounds.[78] In addition, the ability to metabolize aromatic compounds also present in lignocellulosic-based hydrolysates would contribute to an improvement of total carbon conversion. The selected strains, *C. curvatus* ATCC 20509, *R. toruloides* DSM-4444, and *T. guehoae* UCDFST 60-59, were inoculated into YNB medium supplemented with *p*-coumaric acid, ferulic acid, vanillic acid, or 4-hydroxybenzoic acid. All strains were inoculated at the same OD_{600}, and samples were taken over time to monitor potential aromatic compound assimilation (OD_{600} profiles are summarized in **Figure S5**).

Only *R. toruloides* was capable of using all tested lignin-derived acids. It was able to consume 4-hydroxybenozoic

acid and vanillic acid within 72 and 96 hours, respectively. Conversely, full consumption of ferulic and *p*-coumaric acid by *R. toruloides* was only observed after 120 and 168 hours of cultivation, respectively. These results are in agreement with Yaegashi and co-workers, who also recently reported the capability of another *R. toruloides* strain (IFO 0880) of utilizing the same lignin-derived compounds as a sole carbon source.[27] In the case of *C. curvatus* and *T. guehoae* strains, they were only capable of using 4-hydroxybenzoic acid as a sole carbon source, as even after one week of cultivation, no consumption of *p*-coumaric, ferulic, or vanillic acid was observed (**Figure 6**). The consumption profile of 4-hydroxybenzoic acid was different for each strain. Whereas the *R. toruloides* strain fully consumed the aromatic compound within 72 hours, up to 168 hours were required for the other two strains. Moreover, although *C. curvatus* followed a similar consumption profile as *R. toruloides* during the first 48 hours, its consumption slowed considerably for the remainder of the cultivation. In the case of the *T. guehoae* strain, the consumption profile of 4-hydroxybenzoic acid was drastically lower over the course of the whole cultivation (**Figure 6**). Yaguchi *et al*. recently demonstrated not only the capability of *C. curvatus* 20509 to grow on different lignin-derived aromatic compounds, including 4-hydroxybenzoic acid, but also to remain oleaginous during the cultivation, showing its potential as an organism of choice for the production of biofuels from depolymerized lignin.[79] Moreover, the capability of utilizing the tested compounds as a sole carbon source has also been reported for other oleaginous yeast and bacteria.[80, 81] Assimilation of other aromatic compounds via the central intermediates catechol, and protocatechuate via the β-ketoadipate pathway have been demonstrated for different oleaginous yeast species including *Rhodotorula graminis*[82] and *Trichosporon cutaneum*,[83] and oleaginous bacteria such as *Rhodococcus jostii*.[84]

The use of lignin model compounds, including oligomers, polymers and lignin degradation products, represents a fundamental platform to elucidate the metabolism of aromatic compounds by oleaginous microorganisms. However, at the same time, the utilization of real lignin streams, as recently reported for extracted lignin from alkali pretreated corn stover using *Rhodotorula mucilaginosa, Rhodococcus opacus*, and *Rhodococcus jostii* strains,[78, 85-87] will help to assess the feasibility of using oleaginous microorganisms for the biological conversion of biomass-derived lignin to lipids in a more holistic biorefinery.

Lipid extraction

In the interest of demonstrating a fully integrated process, lipid extraction from mixed sugars- and hydrolysate-cultivated yeast was also explored. Harvested yeast cells were washed, lysed with aqueous acid, and extracted with hexane using the method developed by Kruger *et al*.[88] Briefly, the harvested cells were diluted to 8 wt% yeast solids in water and lysed at 170°C for 60 min with 1 wt% H_2SO_4. Following the acid treatment, the lysed cell slurries were extracted with an equal volume of hexane four sequential times, the hexane was evaporated, and the recovered lipids were analyzed for FAME content[89] and compared to the FAME content of the starting cell mass. As shown in **Figure 7**, greater than 90% of the lipids could be recovered from all of the strains by this protocol, whether the yeast was cultivated on mixed sugars or hydrolysate.

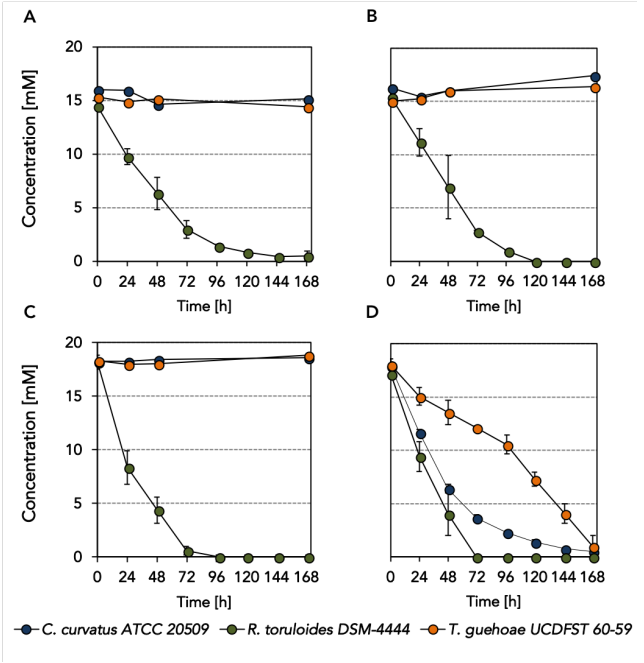

Figure 6. Shake flask cultivations on YNB media supplemented with *p*-coumaric acid (A), ferulic acid (B), vanillic acid (C), or 4-hydroxybenzoic acid (D) as a sole carbon source for *C. curvatus* ATCC 20509, *R. toruloides* DSM-4444, and *T. guehoae* UCDFST 60-59 strains.

Surprisingly, the extraction trend varied significantly across species and cultivation media. In mixed sugars media (**Figure 7**), *C. curvatus* lipids were readily extractable, with 93.7% recovered in the first extraction, and greater than 99% after the second extraction. In contrast, only 43.9% and 38.0% of the lipids from *R. toruloides* and *T. guehoae*, respectively, were recovered in the first extraction, and neither gave a recovery yield above 90% until the fourth extraction. When the cultivation medium was changed to biomass hydrolysate (**Figure 7B**), however, *C. curvatus* lipids became much less extractable, with only 42.7% recovered in the first extraction. Hydrolysate-cultivated *T. guehoae* also exhibited a low recovery yield of 55.5% in the first extraction, while *R. toruloides* exhibited an 83.3% recovery yield.

The reason for these differences is not well understood at this point, but may arise from the stress response of each strain —either the nutrient limitation required for lipid accumulation or toxic components in the hydrolysate.[90-94] It is also possible that the superior ability of *R. toruloides* to utilize aromatic compounds in the hydrolysate, delayed its stress response and subsequent recalcitrance to lipid extraction. The observation that greater than 90% of the lipids could be recovered in all cases suggests that acid hydrolysis is effective across strains and cultivation media, but that different components in the post-lysis slurries may inhibit the hexane extraction. These differences underscore

the importance of integrated studies of full biorefinery process flows, as changes in lipid extractability will affect the size and solvent consumption in the extraction unit operation. Further exploration of these effects is outside the scope of this study, but because of the superior performance of *R. toruloides* in hydrolysate (including a higher capability of inhibitor conversion), the ability of growth on four aromatic compounds as a sole carbon source, and the provision of genetic tools for metabolic engineering strategies, we elected to scale up this strain for conversion of the yeast lipids into diesel blendstock.

Lipid conversion into diesel blendstock

To generate sufficient lipid mass for hydroprocessing experiments, *R. toruloides* was cultivated in mixed sugars media. YNB medium supplemented with an initial composition of 100 g L^{-1} of total sugars (at the same ratio of glucose, xylose, arabinose, and galactose present in DDAP-EH corn stover hydrolysate) was used to perform a 10 L batch cultivation, which was carried out until sugar depletion. The broth was centrifuged, and the yeast pellet was washed with water and stored at -80°C until pretreatment and extraction.

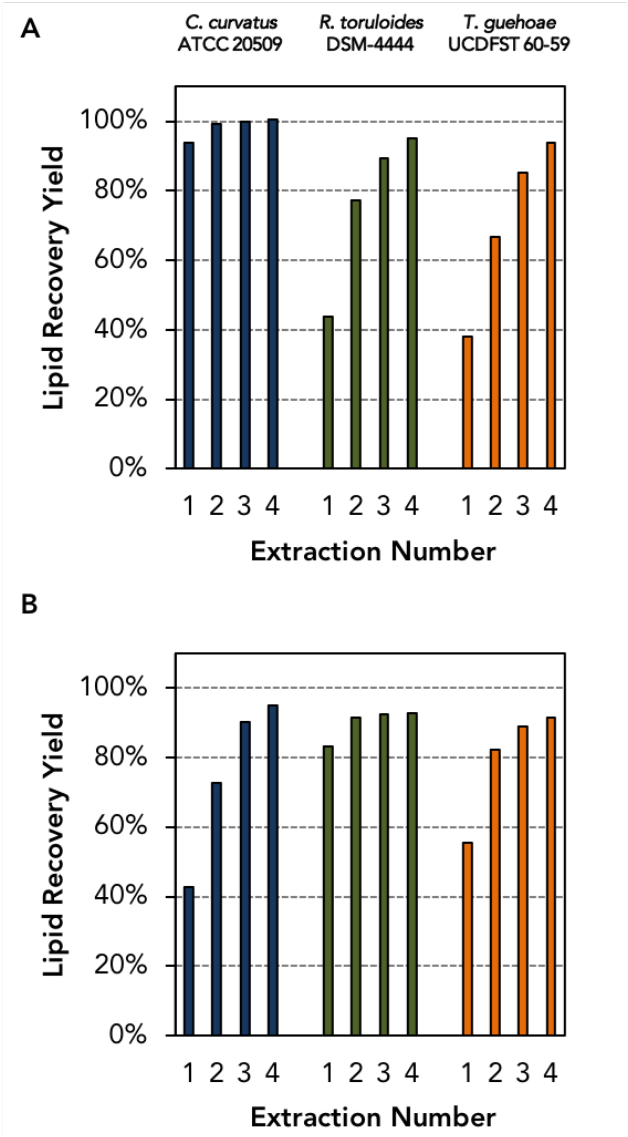

Figure 7. Lipid extraction yields from harvested oleaginous yeast grown in mixed sugars (A) and biomass hydrolysate (B).

Figure 8 shows the steps of the conversion process. Pretreatment was carried out in a Zipperclave reactor in batch mode at an initial concentration of yeast of *ca*. 8% wt, and 1% wt H_2SO_4 at 170°C for one hour. The resulting slurry was transferred to a round bottom flask, and hexane was added to the same initial yeast concentration (8% wt) to perform the lipid extraction step. The system was stirred overnight to facilitate the extraction to the hexane phase. Upon phase separation, the organic phase was transferred into a second round-bottom flask where hexane was evaporated under vacuum, yielding a semi-solid paste at room temperature (**Figure 8B**). The initial color of the lipid extract was orange due to an extraction of carotenoid compounds with the lipids. Although present in relatively small amounts, removal of carotenoids prior to hydrotreating would be advantageous, as they represent a valuable coproduct,[95] and their presence increases the hydrogen consumption due to a high degree of unsaturation.

The lipid extract was dissolved in hexane to be pumped into the hydrotreating reactor (**Figure 8C**). The HDO reaction liquid-phase yields averaged 79.9% through 35 h time-on-stream (TOS). Online GC analysis showed that the reaction reached steady state after about 10 h TOS, after which CO and CO_2 production were around 0.05 and 0.02 g g^{-1} oil, respectively. Similarly, apparent hydrogen consumption averaged roughly 0.01 g H_2 g^{-1} oil (**Figure 9**).

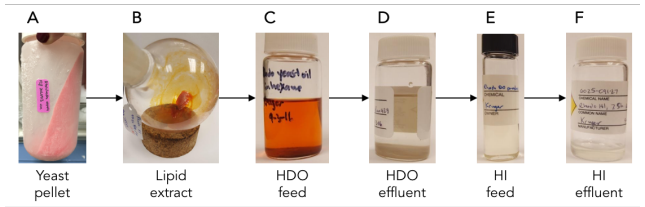

Figure 8. Pictures illustrating the process of lipid conversion into diesel blendstock.

The liquid phase (**Figure 8D**) contained C15-C18 *n*-alkanes, primarily C15 and C17, (two largest peaks in Figure S1A, respectively), indicating that the major pathways for oxygen removal were through decarbonylation and decarboxylation. This is consistent with previous research on lipid deoxygenation over Pd/C catalysts showing C_{n-1} normal alkanes as the primary products from C_n fatty acid chains.[96] Under similar conditions, an oleic acid control reaction without catalyst gave high conversion, but only partial deoxygenation and partial saturation of double bonds.[96] The liquid product also contained lighter and heavier alkanes from cracking and recombination reactions, respectively, which is likely due to the severe conditions of the HDO reactor. Fatty acids are increasingly prone to thermal cracking reactions above 300°C,[97, 98] and the high pressure may be favorable for oligomerization reactions of unsaturated compounds, which

oligomers can then also subsequently crack to yield compounds in the C20-C35 range.

Upon separation of the organic phase and evaporation of the hexane solvent, this mixture of alkanes exhibited a cloud point near room temperature (22.6°C) (**Figure 8E**), but could be kept liquid for prolonged periods by immersing its container in warm water. This mixture of alkanes was hydroisomerized, giving a clear liquid product in 67.9% yield after 7.5 h time-on-stream (**Figure 8F**).

After isomerization, the liquid product initially exhibited a cloud point of 5.6°C, measured by differential scanning calorimetry, which is significantly decreased from the HDO product, reflecting the isomerization of paraffins into isoparaffins (**Figure 10A**), and the cracking of heavier components into diesel and naphtha range components (**Figure 10B** and **Figure S1**). However, the cloud point was higher than expected, and was likely due to the presence of a small fraction of heavy alkanes in the HDO product that were not converted in the HI step. These components formed wax crystals that could be easily filtered out with minimal yield losses by dissolving the HI product in hexane, holding the solution at -20°C and filtering while cold. After this cold filtration step, the cloud point was measured to be -14.5°C.

Simulated distillation of the HI product yielded the boiling curve where approximately 75% of the product was in the diesel range, using a cutoff temperature of 175°C to distinguish between gasoline and diesel fractions. Similarly, the T90 of the material was within the acceptable range (282-338°C) for No. 2 diesel fuel (**Figure 10C**).

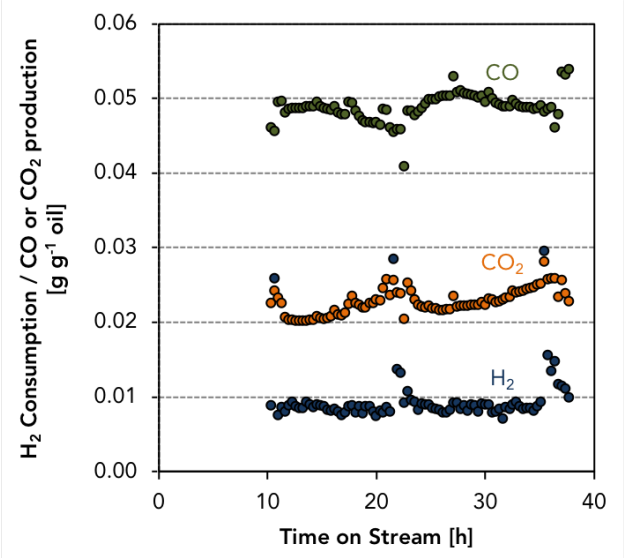

Figure 9. De-CO_x product formation and H_2 consumption during R. Toruloides oil deoxygenation. Reaction conditions: 450 °C, 1300 psig H_2, LHSV = 1 hr^{-1}.

The hydrotreating conditions were relatively harsh compared to what has been required for deoxygenation of lipid feedstocks in previously reported studies.[99] The conditions used in the present experiments were informed by our previous work with crude, hexane extracted algal lipids, which required high temperature and pressure to remove impurities, particularly nitrogen.[96] Since the nitrogen content of the yeast lipid extract was unknown,

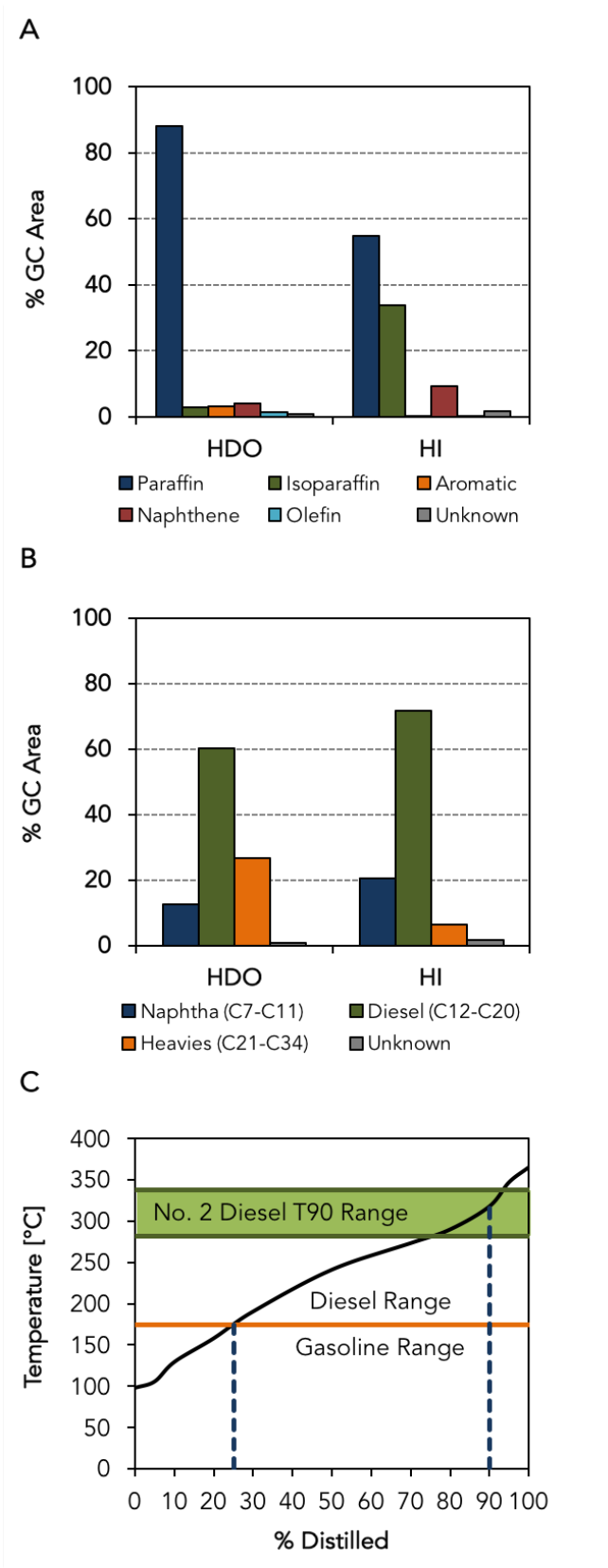

Figure 10. *R. toruloides* DSM-4444 strain lipid conversion. Hydrocarbon speciation (A), and hydrocarbon distribution according to molecular weight (B) of hydrodeoxygenation (HDO) and hydroisomerization (HI) liquid product characterization by GC/MS. Simulated distillation curve measured for deoxygenated, isomerized product (C).

conservative conditions were employed to ensure a successful conversion to diesel blendstock. Therefore, conditions could likely be improved if more detailed analysis of the yeast lipid extracts suggested low impurity levels. The origin of the heavy fraction is not well understood at this point, but may be partly due to recombination of thermal decomposition products.[100]

Discussion

In this work, we have demonstrated an integrated, bench-scale process for converting lignocellulosic sugars in an industrially-relevant hydrolysate stream to a fungible diesel blendstock by converting the sugars, both pentoses and hexoses, to a lipid fuel precursor in oleaginous yeast, lysing the yeast cells to recover the lipids via hexane extraction, deoxygenation of the crude recovered lipids over a Pd/C catalyst, and isomerizing the deoxygenated lipids over a Pt/SAPO-11 catalyst. Accordingly, this work demonstrates the relatively high technical readiness level of the combined biological-catalytic processing of the sugars-lipids-fuel approach to drop-in cellulosic biofuels. Previous economic analyses have shown that this approach is likely capable of producing biofuel with a minimum selling price in the range of $4-5/gallon of gasoline equivalent.[49, 88] Some of the main contributing factors to this selling price are the relatively expensive cultivation of the yeast due to strict aerobic requirements, the relatively low metabolic yield of sugars to lipids, the ongoing need for acid (and alkali for post-extraction neutralization) to lyse the cells, solvent losses in the extraction step, and capital costs for the hydroprocessing reactors due to the relatively severe conditions employed here. While the furthest downstream process expenses can likely be improved by judicious engineering (e.g., increasing lipid recovery yields by using a continuous countercurrent extraction column, decreasing solvent losses by using a multi-component extractant, and decreasing hydroprocessing severity by catalyst and process development), the mid- and upstream processes are likely to remain significant cost drivers due to the fundamental nature of lipids as an aerobic intracellular product. At production scale, microbial performance is often highly dependent on mass and heat transfer. High mixing times lead to gradients in temperature, pH, gradients in nutrients, substrates and gas, as well as the hydrostatic pressure in the bioreactor. These effects may become even more acute when the cellular pathway is oxygen dependent, as it is for lipid production.[101, 102] Moreover, the accumulation of lipids as an intracellular product introduces two key challenges: a significant fraction of sugars is converted to cell mass instead of fuel precursor, and the cells must be lysed to release and recover the lipids.

There are multiple scientific approaches to overcome these challenges. First, the use of a combined approach to screen for strains with high lipid production capabilities in a short period of time will continue to be essential to increase the size of the screening. Over the last years, researchers have used an initial qualitative assessment, such as thin layer chromatography[103] or Nile Red staining,[104] with a quantitative determination of lipid production to identify superior candidate strains for the production of lipids. In addition, lipid accumulation can be promoted by bioprocessing optimization. The use of fed batch strategies can uncouple the growth phase and the lipid accumulation phase by having a substrate limited in nitrogen or other nutrient during the feeding period.[23] Second, the yeast may be engineered to secrete lipid fuel precursors, such as fatty alcohols[105] or aldehydes, despite the fact that metabolic engineering of non-model organisms has proven to be much more difficult. A stronger preference for non-homologous end-joining and low activity for integration via homologous recombination is presumably the cause, since many of the genetic tools rely on the high capacity of the microorganism to undergo homologous recombination (for a recent review see Shi and Zhao[106]). Third, the yeast may be triggered to autolyse instead of requiring an explicit set of unit operations for cell lysis. This activity has been observed in *S. cerevisiae* strains employed to enhance the flavor profile in sparkling wine,[107] but also facilitating the polyhydroxyalkanoate recovery in the bacterium *Pseudomonas putida*.[108] Fourth, the yeast may be cultivated as a biofilm instead of in a bioreactor to enhance gas transfer rates to the growing yeast in a less expensive manner than bubbling compressed air through a growth medium. This approach would also decrease the energy intensity of the harvesting step because the yeast could be scraped off the biofilm instead of being processed in a centrifuge. Fifth, the lipid fraction of yeast biomass which does not consist of lipid fuel precursors could be valorised by recovering coproducts (e.g., sterols, trehalose or carotenoid pigments).[109]

It is also worth noting that the relatively low metabolic yield of sugars to lipids is offset by the resemblance of lipids to a finished fuel. That is, the typical metabolic yield of sugars to lipids of 0.24 g lipid/g sugar combined with a theoretical lipid recovery yield of 100% and a theoretical deoxygenation/hydroisomerization efficiency of 85-90% (depending on the speciation of the fatty acid chains and the chemistry of oxygen removal as H_2O, CO, or CO_2) to give a theoretical sugar-to-fuel yield of roughly 0.2 g fuel/g sugar input. The high conversion efficiencies are possible because the lipids contain only ~10% oxygen. For comparison, ethanol can be produced at a theoretical metabolic yield of 0.51 g/g sugar (commercial plants using sugar cane can operate at roughly 90% of this value),[110, 111] but contains ~35% oxygen. Conversion of ethanol into hydrocarbon fuels frequently results in primarily gasoline-range mixtures,[112-114] although a few efforts have focused on producing diesel-range materials. In general, these approaches involve dehydration to ethylene and oligomerization to the appropriate carbon number range. The oligomerization of light olefins is typically able to generate 50-70% yield to diesel range hydrocarbons.[115-117] Assuming a 70% efficient ethylene oligomerization strategy

to produce diesel-range carbon chains, the overall efficiency would be ~0.2 g diesel-range fuel/g sugar from ethanol. Thus, overall, the lipid pathway for cellulosic biofuels is in the range of alcohol-based pathways in terms of mass efficiencies, but further process development is necessary to improve the economics of the overall process.

Moreover, we have demonstrated, consistent with several previous studies, that oleaginous yeasts were not only able to metabolize several of the inhibitors present in lignocellulosic-based hydrolysates, but also to use aromatic compounds as a sole carbon source. However, there is a need of systematic studies to elucidate the aromatic catabolic pathways in these oleaginous yeasts as it has been conducted in aromatic degrading bacteria.[77, 118, 119] Also, improved genome and functional annotation would also allow a more comprehensive understanding of the multiple lignin degradation pathways in oleaginous yeast strains. Ultimately, in a broader context such as in biorefineries, polysaccharide and lignin valorization in parallel or simultaneously will be key to maximize the economic profitability of lignocellulosic biorefining.

Experimental

Material and Methods section can be found in Electronic Supplementary Information.

Conflict of interests

There are no conflicts to declare.

Acknowledgements

This work was authored by Alliance for Sustainable Energy, LLC, the manager and operator of the National Renewable Energy Laboratory for the U.S. Department of Energy (DOE) under Contract No. DE-AC36-08GO28308. Funding was provided by the DOE Energy Efficiency and Renewable Energy (EERE) Bioenergy Technologies Office (BETO). Dan Schell and the team at NREL's Biochemical Conversion Pilot Plant are gratefully acknowledged for providing DDAP-EH corn stover hydrolysate. We thank Earl Christensen for analysis of the DO and HI products. We thank Nancy Dowe, Thieny Trinh, and Andrew Lowell for initiating an earlier version of this study and for helpful discussions, and Eric Knoshaug for providing suggestions for several oleaginous yeast strains to examine. The views expressed in the article do not necessarily represent the views of the DOE or the U.S. Government. The U.S. Government retains and the publisher, by accepting the article for publication, acknowledges that the U.S. Government retains a nonexclusive, paid-up, irrevocable, worldwide license to publish or reproduce the published form of this work, or allow others to do so, for U.S. Government purposes.

References

1. A. Ragauskas, C. Williams, B. Davison, G. Britovsek, J. Cairney, C. Eckert, W. Frederick, J. Hallett, D. Leak, C. Liotta, J. Mielenz, R. Murphy, R. Templer and T. Tschaplinski, *Science*, 2006, **311**, 484 - 489.
2. L. R. Lynd, M. S. Laser, D. Bransby, B. E. Dale, B. Davison, R. Hamilton, M. Himmel, M. Keller, J. D. McMillan and J. Sheehan, *Nature Biotechnology*, 2008, **26**, 169-172.
3. G. Stephanopoulos, *Science*, 2007, **315**, 801-804.
4. J. N. Chheda, G. W. Huber and J. A. Dumesic, *Angewandte Chemie International Edition*, 2007, **46**, 7164-7183.
5. S. K. Lee, H. Chou, T. S. Ham, T. S. Lee and J. D. Keasling, *Current Opinion in Biotechnology*, 2008, **19**, 556-563.
6. H. Alper and G. Stephanopoulos, *Nature Reviews Microbiology*, 2009, **7**, 715-723.
7. M. R. Connor and J. C. Liao, *Current Opinion in Biotechnology*, 2009, **20**, 307-315.
8. J. C. Serrano-Ruiz and J. A. Dumesic, *Energy & Environmental Science*, 2011, **4**, 83-99.
9. S. Van de Vyver, J. Geboers, P. A. Jacobs and B. F. Sels, *ChemCatChem*, 2011, **3**, 82-94.
10. P. P. Peralta-Yahya, F. Zhang, S. B. del Cardayre and J. D. Keasling, *Nature*, 2012, **488**, 320-328.
11. J. C. Serrano-Ruiz, R. M. West and J. A. Dumesic, *Annual Review of Chemical and Biomolecular Engineering*, 2010, **1**, 79-100.
12. P. Mäki-Arvela, I. Kubickova, M. Snåre, K. Eränen and D. Y. Murzin, *Energy & Fuels*, 2007, **21**, 30-41.
13. M. K. Akhtar, N. J. Turner and P. R. Jones, *Proceedings of the National Academy of Sciences*, 2013, **110**, 87-92.
14. M. Snåre, I. Kubičková, P. Mäki-Arvela, K. Eränen and D. Y. Murzin, *Industrial & Engineering Chemistry Research*, 2006, **45**, 5708-5715.
15. E. J. Steen, Y. Kang, G. Bokinsky, Z. Hu, A. Schirmer, A. McClure, S. B. del Cardayre and J. D. Keasling, *Nature*, 2010, **463**, 559.
16. V. Sànchez Nogué and K. Karhumaa, *Biotechnology Letters*, 2015, **37**, 761-772.
17. J. Blazeck, A. Hill, L. Liu, R. Knight, J. Miller, A. Pan, P. Otoupal and H. S. Alper, *Nature Communications*, 2014, **5**.
18. M. Tai and G. Stephanopoulos, *Metabolic Engineering*, 2013, **15**, 1-9.
19. Y. A. Tsigie, C.-Y. Wang, C.-T. Truong and Y.-H. Ju, *Bioresource Technology*, 2011, **102**, 9216-9222.
20. K. Qiao, S. H. Imam Abidi, H. Liu, H. Zhang, S. Chakraborty, N. Watson, P. Kumaran Ajikumar and G. Stephanopoulos, *Metabolic Engineering*, 2015, **29**, 56-65.
21. M. Thiru, S. Sankh and V. Rangaswamy, *Bioresource Technology*, 2011, **102**, 10436-10440.
22. J. Zhang, X. Fang, X.-L. Zhu, Y. Li, H.-P. Xu, B.-F. Zhao, L. Chen and X.-D. Zhang, *Biomass and Bioenergy*, 2011, **35**, 1906-1911.
23. Y. Li, Z. K. Zhao and F. Bai, *Enzyme and Microbial Technology*, 2007, **41**, 312-317.

24. Z. Zhu, S. Zhang, H. Liu, H. Shen, X. Lin, F. Yang, Y. J. Zhou, G. Jin, M. Ye, H. Zou and Z. K. Zhao, *Nature Communications*, 2012, **3**, 1112.
25. C. Hu, X. Zhao, J. Zhao, S. Wu and Z. K. Zhao, *Bioresource Technology*, 2009, **100**, 4843-4847.
26. S. Wu, X. Zhao, H. Shen, Q. Wang and Z. K. Zhao, *Bioresource Technology*, 2011, **102**, 1803-1807.
27. J. Yaegashi, J. Kirby, M. Ito, J. Sun, T. Dutta, M. Mirsiaghi, E. R. Sundstrom, A. Rodriguez, E. Baidoo, D. Tanjore, T. Pray, K. Sale, S. Singh, J. D. Keasling, B. A. Simmons, S. W. Singer, J. K. Magnuson, A. P. Arkin, J. M. Skerker and J. M. Gladden, *Biotech. Biofuels*, 2017, **10**, 241.
28. C. Saenge, B. Cheirsilp, T. T. Suksaroge and T. Bourtoom, *Process Biochemistry*, 2011, **46**, 210-218.
29. E. R. Easterling, W. T. French, R. Hernandez and M. Licha, *Bioresource Technology*, 2009, **100**, 356-361.
30. G. Zhang, W. T. French, R. Hernandez, E. Alley and M. Paraschivescu, *Biomass and Bioenergy*, 2011, **35**, 734-740.
31. Z. Gong, Q. Wang, H. Shen, C. Hu, G. Jin and Z. K. Zhao, *Bioresource Technology*, 2012, **117**, 20-24.
32. C. Huang, X.-F. Chen, X.-Y. Yang, L. Xiong, X.-Q. Lin, J. Yang, B. Wang and X.-D. Chen, *Appl Biochem Biotechnol*, 2014, **172**, 2197-2204.
33. X. Zhao, X. Kong, Y. Hua, B. Feng and Z. K. Zhao, *European Journal of Lipid Science and Technology*, 2008, **110**, 405-412.
34. P. Xu, K. Qiao, W. S. Ahn and G. Stephanopoulos, *Proceedings of the National Academy of Sciences*, 2016, **113**, 10848-10853.
35. K. Qiao, T. M. Wasylenko, K. Zhou, P. Xu and G. Stephanopoulos, *Nature Biotechnology*, 2017, **35**, 173.
36. S. Zhang, M. Ito, J. M. Skerker, A. P. Arkin and C. V. Rao, *Applied Microbiology and Biotechnology*, 2016, **100**, 9393-9405.
37. M. S. Davis, J. Solbiati and J. E. Cronan, *Journal of Biological Chemistry*, 2000, **275**, 28593-28598.
38. X. Lu, H. Vora and C. Khosla, *Metabolic Engineering*, 2008, **10**, 333-339.
39. T. Liu, H. Vora and C. Khosla, *Metabolic Engineering*, 2010, **12**, 378-386.
40. J. Clomburg and R. Gonzalez, *Applied Microbiology and Biotechnology*, 2010, **86**, 419-434.
41. R. M. Lennen, D. J. Braden, R. M. West, J. A. Dumesic and B. F. Pfleger, *Biotechnology and Bioengineering*, 2010, **106**, 193-202.
42. P. Handke, S. A. Lynch and R. T. Gill, *Metabolic Engineering*, 2011, **13**, 28-37.
43. W. Runguphan and J. D. Keasling, *Metabolic Engineering*, 2014, **21**, 103-113.
44. N. A. Buijs, V. Siewers and J. Nielsen, *Current Opinion in Chemical Biology*, 2013, **17**, 480-488.
45. X. Tang, H. Feng and W. N. Chen, *Metabolic Engineering*, 2013, **16**, 95-102.
46. J. O. Valle-Rodríguez, S. Shi, V. Siewers and J. Nielsen, *Applied Energy*, 2014, **115**, 226-232.
47. I. R. Sitepu, L. A. Garay, R. Sestric, D. Levin, D. E. Block, J. B. German and K. L. Boundy-Mills, *Biotechnology Advances*, 2014, **32**, 1336-1360.
48. J. M. Ageitos, J. A. Vallejo, P. Veiga-Crespo and T. G. Villa, *Applied Microbiology and Biotechnology*, 2011, **90**, 1219-1227.
49. M. J. Biddy, R. Davis, D. Humbird, L. Tao, N. Dowe, M. T. Guarnieri, J. G. Linger, E. M. Karp, D. Salvachúa, D. R. Vardon and G. T. Beckham, *ACS Sustainable Chemistry & Engineering*, 2016, **4**, 3196-3211.
50. R. Davis, L. Tao, E. Tan, M. J. Biddy, G. T. Beckham, C. Scarlata, J. Jacobson, K. Cafferty, J. Ross, J. Lukas, D. Knorr and P. Schoen, *Process Design and Economics for the Conversion of Lignocellulosic Biomass to Hydrocarbons: Dilute-Acid Prehydrolysis and Enzymatic Hydrolysis Deconstruction of Biomass to Sugars and Biological Conversion of Sugars to Hydrocarbons*, NREL, Golden, CO, 2013.
51. P. J. Slininger, B. S. Dien, C. P. Kurtzman, B. R. Moser, E. L. Bakota, S. R. Thompson, P. J. O'Bryan, M. A. Cotta, V. Balan, M. Jin, L. d. C. Sousa and B. E. Dale, *Biotechnology and Bioengineering*, 2016, **113**, 1676-1690.
52. B. S. Dien, P. J. Slininger, C. P. Kurtzman, B. R. Moser and P. J. O'Bryan, *AIMS Environmental Science*, 2016, **3**, 1-20.
53. J. P. Sampaio, in *The Yeasts (Fifth Edition)*, eds. J. W. Fell and T. Boekhout, Elsevier, London, 2011, pp. 1873-1927.
54. J.-E. Lee, P. V. Vadlani and D. Min, *Journal of Sustainable Bioenergy Systems*, 2017, **7**, 36-50.
55. X. Yu, Y. Zheng, K. M. Dorgan and S. Chen, *Bioresource Technology*, 2011, **102**, 6134-6140.
56. Y.-H. Chang, K.-S. Chang, C.-L. Hsu, L.-T. Chuang, C.-Y. Chen, F.-Y. Huang and H.-D. Jang, *Fuel*, 2013, **105**, 711-717.
57. Y.-H. Chang, K.-S. Chang, C.-F. Lee, C.-L. Hsu, C.-W. Huang and H.-D. Jang, *Biomass and Bioenergy*, 2015, **72**, 95-103.
58. Q. Fei, M. O'Brien, R. Nelson, X. Chen, A. Lowell and N. Dowe, *Biotech. Biofuels*, 2016, **9**, 130.
59. X. Zhao, S. Wu, C. Hu, Q. Wang, Y. Hua and Z. K. Zhao, *Journal of Industrial Microbiology & Biotechnology*, 2010, **37**, 581-585.
60. J. Brandenburg, J. Blomqvist, J. Pickova, N. Bonturi, M. Sandgren and V. Passoth, *Yeast*, 2016, **33**, 451-462.
61. J. Wang, Q. Gao, H. Zhang and J. Bao, *Bioresource Technology*, 2016, **218**, 892-901.
62. X. Tang, H. Chen, Y. Q. Chen, W. Chen, V. Garre, Y. Song and C. Ratledge, *PLOS ONE*, 2015, **10**, e0128396.
63. D. Hardman, D. McFalls and S. Fakas, *Yeast*, 2017, **34**, 83-91.
64. S. Fakas, *Engineering in Life Sciences*, 2017, **17**, 292-302.

65. J. R. Petrie, T. Vanhercke, P. Shrestha, A. El Tahchy, A. White, X.-R. Zhou, Q. Liu, M. P. Mansour, P. D. Nichols and S. P. Singh, *PLOS ONE*, 2012, **7**, e35214.
66. G. M. Carman, *Biochemical Society Transactions*, 2005, **33**, 1150-1153.
67. R. Plaggenborg, J. Overhage, A. Loos, J. A. C. Archer, P. Lessard, A. J. Sinskey, A. Steinbüchel and H. Priefert, *Applied Microbiology and Biotechnology*, 2006, **72**, 745.
68. S. Mathew and T. E. Abraham, *Critical Reviews in Microbiology*, 2006, **32**, 115-125.
69. P. Wang, J. E. Brenchley and A. E. Humphrey, *Biotechnology Letters*, 1994, **16**, 977-982.
70. F. Koopman, N. Wierckx, J. H. de Winde and H. J. Ruijssenaars, *Proceedings of the National Academy of Sciences*, 2010, **107**, 4919-4924.
71. H. Ran, J. Zhang, Q. Gao, Z. Lin and J. Bao, *Biotech. Biofuels*, 2014, **7**, 51.
72. D. Feldman, D. J. Kowbel, N. L. Glass, O. Yarden and Y. Hadar, *Biotech. Biofuels*, 2015, **8**, 63.
73. C. Huang, H. Wu, T. J. Smith, Z. j. Liu, W. Y. Lou and M. h. Zong, *Biotechnology Letters*, 2012, **34**, 1637-1642.
74. I. Sárvári Horváth, C. J. Franzén, M. J. Taherzadeh, C. Niklasson and G. Lidén, *Applied and Environmental Microbiology*, 2003, **69**, 4076-4086.
75. N. Wierckx, F. Koopman, L. Bandounas, J. H. De Winde and H. J. Ruijssenaars, *Microbial Biotechnology*, 2010, **3**, 336-343.
76. M. T. Guarnieri, M. Ann Franden, C. W. Johnson and G. T. Beckham, *Metabolic Engineering Communications*, 2017, **4**, 22-28.
77. G. T. Beckham, C. W. Johnson, E. M. Karp, D. Salvachúa and D. R. Vardon, *Current Opinion in Biotechnology*, 2016, **42**, 40-53.
78. D. Salvachúa, E. M. Karp, C. T. Nimlos, D. R. Vardon and G. T. Beckham, *Green Chem.*, 2015, **17**, 4951-4967.
79. A. Yaguchi, A. Robinson, E. Mihealsick and M. Blenner, *Microbial Cell Factories*, 2017, **16**, 206.
80. J. P. Sampaio, *Canadian Journal of Microbiology*, 1999, **45**, 491-512.
81. S. A. Shields-Menard, M. AmirSadeghi, M. Green, E. Womack, D. L. Sparks, J. Blake, M. Edelmann, X. Ding, B. Sukhbaatar, R. Hernandez, J. R. Donaldson and T. French, *International Biodeterioration and Biodegradation*, 2017, **121**, 79-90.
82. D. R. Durham, C. G. McNamee and D. B. Stewart, *Journal of Bacteriology*, 1984, **160**, 771-777.
83. A. Gaal and H. Y. Neujahr, *Journal of Bacteriology*, 1979, **137**, 13-21.
84. S. Amara, N. Seghezzi, H. Otani, C. Diaz-Salazar, J. Liu and L. D. Eltis, *Scientific Reports*, 2016, **6**, 24985.
85. A. Rodriguez, D. Salvachúa, R. Katahira, B. A. Black, N. S. Cleveland, M. Reed, H. Smith, E. E. K. Baidoo, J. D. Keasling, B. A. Simmons, G. T. Beckham and J. M. Gladden, *ACS Sustainable Chemistry & Engineering*, 2017, **5**, 8171-8180.
86. R. K. Le, T. Wells Jr, P. Das, X. Meng, R. J. Stoklosa, A. Bhalla, D. B. Hodge, J. S. Yuan and A. J. Ragauskas, *RSC Advances*, 2017, **7**, 4108-4115.
87. Y. He, X. Li, H. Ben, X. Xue and B. Yang, *ACS Sustainable Chemistry & Engineering*, 2017, **5**, 2302-2311.
88. J. S. Kruger, N. S. Cleveland, R. Y. Yeap, T. Dong, K. J. Ramirez, N. J. Nagle, A. C. Lowell, G. T. Beckham, J. D. McMillan and M. J. Biddy, *ACS Sustainable Chemistry & Engineering*, 2018, DOI: 10.1021/acssuschemeng.7b01874.
89. L. M. L. Laurens, M. Quinn, S. Van Wychen, D. W. Templeton and E. J. Wolfrum, *Analytical and Bioanalytical Chemistry*, 2012, **403**, 167-178.
90. M. K. Conway, D. Grunwald and W. Heideman, *G3: Genes|Genomes|Genetics*, 2012, **2**, 1003-1017.
91. E. Van Donk, M. Lürling, D. O. Hessen and G. M. Lokhorst, *Limnology and Oceanography*, 1997, **42**, 357-364.
92. T. Dong, S. Van Wychen, N. Nagle, P. T. Pienkos and L. M. L. Laurens, *Algal Research*, 2016, **18**, 69-77.
93. H. G. Gerken, B. Donohoe and E. P. Knoshaug, *Planta*, 2013, **237**, 239-253.
94. M. Werner-Washburne, E. Braun, G. C. Johnston and R. A. Singer, *Microbiological Reviews*, 1993, **57**, 383-401.
95. Y.-K. Park, J.-M. Nicaud and R. Ledesma-Amaro, *Trends in Biotechnology*, 2017.
96. J. S. Kruger, E. D. Christensen, T. Dong, S. Van Wychen, G. M. Fioroni, P. T. Pienkos and R. L. McCormick, *Energy & Fuels*, 2017, **31**, 10946-10953.
97. M. Omidghane, E. Jenab, M. Chae and D. C. Bressler, *Energy & Fuels*, 2017, **31**, 9446-9454.
98. R. O. Idem, S. P. R. Katikaneni and N. N. Bakhshi, *Energy & Fuels*, 1996, **10**, 1150-1162.
99. H. J. Robota, J. C. Alger and L. Shafer, *Energy & Fuels*, 2013, **27**, 985-996.
100. J. Asomaning, P. Mussone and D. C. Bressler, *Journal of Analytical and Applied Pyrolysis*, 2014, **105**, 1-7.
101. D. McMillan James and T. Beckham Gregg, *Microbial Biotechnology*, 2016, **10**, 40-42.
102. F. Delvigne and H. Noorman, *Microbial Biotechnology*, 2017, **10**, 685-687.
103. D. Lamers, N. van Biezen, D. Martens, L. Peters, E. van de Zilver, N. Jacobs-van Dreumel, R. H. Wijffels and C. Lokman, *BMC Biotechnology*, 2016, **16**, 45.
104. R. Poontawee, W. Yongmanitchai and S. Limtong, *Process Biochemistry*, 2017, **53**, 44-60.
105. S. Fillet, J. Gibert, B. Suarez, A. Lara, C. Ronchel and J. L. Adrio, *Journal of Industrial Microbiolology & Biotechnology*, 2015, **42**, 1463-1472.

106. S. Shi and H. Zhao, *Frontiers in Microbiology*, 2017, **8**, 2185.
107. A. J. Martínez-Rodríguez and E. Pueyo, in *Wine chemistry and biochemistry*, eds. M. V. Moreno-Arribas and C. Polo, Springer-Verlag, New York, 2009, DOI: 10.1007/978-0-387-74118-5, ch. 3A, pp. 61-80.
108. V. Martínez, P. García, J. L. García and M. A. Prieto, *Microbial Biotechnology*, 2011, **4**, 533-547.
109. O. Pastinen, A. Nyyssölä, V. Pihlajaniemi and M. H. Sipponen, *Process Biochemistry*, 2017, **58**, 217-223.
110. B. E. Della-Bianca, T. O. Basso, B. U. Stambuk, L. C. Basso and A. K. Gombert, *Applied Microbiology and Biotechnology*, 2013, **97**, 979-991.
111. A. K. Gombert and A. J. A. van Maris, *Current Opinion in Biotechnology*, 2015, **33**, 81-86.
112. V. F. Tret'yakov, Y. I. Makarfi, K. V. Tret'yakov, N. A. Frantsuzova and R. M. Talyshinskii, *Catalysis in Industry*, 2010, **2**, 402-420.
113. N. Viswanadham, S. K. Saxena, J. Kumar, P. Sreenivasulu and D. Nandan, *Fuel*, 2012, **95**, 298-304.
114. J. J. Lovón-Quintana, J. K. Rodriguez-Guerrero and P. G. Valença, *Applied Catalysis A: General*, 2017, **542**, 136-145.
115. O. Muraza, *Industrial & Engineering Chemistry Research*, 2015, **54**, 781-789.
116. *US Pat.,* 20070287873A1, 2006.
117. *WO Pat.,* 2016160839A1, 2015.
118. E. Masai, Y. Katayama and M. Fukuda, *Bioscience, Biotechnology, and Biochemistry*, 2007, **71**, 1-15.
119. N. Kamimura, K. Katakahashi, K. Mori, T. Araki, M. Fujita, Y. Higuchi and E. Masa, *Environmental Microbiology Reports*, 2017, **9**, 679-705.

Green Chemistry

PAPER

View Article Online
View Journal | View Issue

Integrated diesel production from lignocellulosic sugars via oleaginous yeast†

Violeta Sànchez i Nogué[1§], Brenna A. Black[2§], Jacob S. Kruger[1§], Christine A. Singer[1], Kelsey J. Ramirez[2], Michelle L. Reed[2], Nicholas S. Cleveland[1], Emily R. Singer[1], Xiunan Yi[1], Rou Yi Yeap[1], Jeffrey G. Linger[1], and Gregg T. Beckham[1,*]

Abstract: Oleaginous microbes are promising platform strains for the production of renewable diesel and fatty-acid derived chemicals given their innate capacity to produce high lipid yields from lignocellulose-derived sugars. Substantial efforts have been conducted to engineer model oleaginous yeasts primarily on model feedstocks, but to enable lipid production from biomass, judicious strain selection based on phenotypes beneficial for processing, performance on realistic feedstocks, and process integration aspects from sugars to fuels should be examined holistically. To that end, here we report the bench-scale production of diesel blendstock using a biological-catalytic hybrid process based on oleaginous yeast. This work includes flask screening of 31 oleaginous yeast strains, evaluated based on baseline lipid profiles and sugar consumption with corn stover hydrolysate. Three strains were down-selected for bioreactor performance evaluation. The cultivation results reveal that *Cryptococcus curvatus* ATCC 20509 and *Rhodosporodium toruloides* DSM-4444 exhibit equivalent fatty acid methyl ester (FAME) yield (0.24 g g^{-1}), whereas the highest overall FAME productivity (0.22 g L^{-1} h^{-1}) was obtained with *C. curvatus,* and *R. toruloides* displayed the highest final FAME titer (23.3 g L^{-1}). Time-resolved lipid profiling (including neutral and polar lipid classing) demonstrated triacylglycerol accumulation as the predominant lipid class in all strains. When evaluating tolerance mechanisms to inhibitory compounds, all strains can reduce and oxidize 5-(hydroxymethyl)furfural, illustrating parallel detoxification mechanisms. The *R. toruloides* strain is also capable of growth on four aromatic compounds as a sole carbon source, suggesting its use as a strain for simultaneous sugar and lignin conversion. Lipids from *R. toruloides* were recovered using a mild acid treatment and extraction, hydrogenated, and isomerized to produce a renewable diesel blendstock. The blendstock exhibited a cloud point of -14.5°C and simulated distillation showed that approximately 75% of the product was in the diesel range with a T90 consistent with No. 2 diesel fuel. Taken together, these results demonstrate an integrated process for renewable diesel production, identify oleaginous strains for further development, and highlight opportunities for improvements to an oleaginous microbial platform for the production of renewable diesel blendstock.

1. National Bioenergy Center, National Renewable Energy Laboratory, Golden CO 80401
2. Biosciences Center, National Renewable Energy Laboratory, Golden CO 80401 USA
§ Authors contributed equally to this work.
** gregg.beckham@nrel.gov*
† Electronic Supplementary Information (ESI) available: Materials and methods, strains used in this study, triacylglycerols and polar lipid speciation, sugar consumption profiles on mock hydrolysate, and growth profiles on aromatic compounds.

Introduction

The continued drive towards renewable transportation fuels will rely on lignocellulosic biomass as a primary feedstock.[1] Over the last several decades, a massive body of work has been conducted towards the development and deployment of lignocellulosic ethanol, especially accelerated in the last decade, and now pioneer plants are emerging, albeit slowly and not without serious technical challenges at the industrial scale.[2] Beyond ethanol production, there is a need for the production of a more comprehensive renewable fuels portfolio to satisfy the diesel, jet fuel, and gasoline markets. Many conversion pathways are being evaluated today to produce hydrocarbon fuels from lignocellulosic biomass. These pathways include multiple deconstruction technologies to produce biomass-derived sugars followed by biological, catalytic, or hybrid biological-catalytic approaches to upgrade sugars to fuel molecules.[3-9]

Biological routes to upgrade sugars directly to fuels beyond ethanol are quite varied. Peralta-Yahya *et al.* broadly categorized advanced biofuels directly available from biological routes according to their respective metabolic pathway as alcohol, fatty acid, isoprenoid, and polyketide-derived fuels.[10] Certainly other biologically derived intermediates can be produced outside of this categorization that can then be catalytically converted to fuels, but the catalytic steps are usually more involved than simple hydrogenation or hydrodeoxygenation reactions

(e.g., in the case of farnesene to farnesane).[11] To date, fuel precursors derived from fatty acid biosynthesis in particular have received significant attention, given that many microbes produce lipids in the C16-C20 range, which is an ideal carbon chain length for diesel. Fatty acids have to be either biologically or catalytically converted to esters, alcohols, or preferably branched alkanes before being used as diesel.[12-15]

For any given biotechnological application, microorganism selection will dictate the challenges faced during process development. In the case of lipid production as a diesel blendstock, selection among oleaginous microorganisms for strains with high flux would be highly beneficial, as they naturally accumulate a considerable fraction of their cell weight as lipids, and its composition is generally quite similar to that of common biodiesel feedstock. Moreover, the use of lignocellulosic biomass as a feedstock ideally demands for two additional crucial traits which will potentially accelerate the development to economic feasibility: i) the capability of the organism to simultaneously consume all present sugars, including hexoses and pentoses, and ii) a high tolerance to lignocellulosic-derived inhibitors present in the hydrolysates.[16] Given the growing interest in the production of diesel-range hydrocarbons from renewable feedstocks, many oleaginous microbes have been well studied in the last decade, including *Yarrowia lipolytica*,[17-20] *Cryptococcus curvatus*,[21, 22] *Rhodosporidium toruloides*,[23-27] *Rhodotorula glutinis* (the anamorph of *R. toruloides*),[28-30] and *Lipomyces starkeyi*[31-33] as they naturally possess several of these desired traits. Oleaginous microbes are typically not as genetically tractable as model bacteria and yeast, but metabolic engineering in *Y. lipolytica* has recently led to dramatic improvements in lipid titer, rate, and yield on clean sugars.[17, 20, 34, 35] Significant improvements in genetic engineering strategies to increase the expression of enzymes involved in different aspects of lipid biosynthesis has also been accomplished in *R. toruloides*.[36] As an alternative, many studies focusing on fatty acid-derived fuels have examined metabolic engineering strategies to increase production of fatty acids (mainly triacylglycerides) in model microorganisms such as *Saccharomyces cerevisiae* or *Escherichia coli*.[37-46] These studies have led to substantially higher lipid yields in these model organisms, but carbon flux is still quite limited relative to oleaginous microorganisms, which naturally accumulate lipids intracellularly as a stress response during nutrient deprivation.[47, 48]

Despite exciting advances in the production of microbial lipids, significant work remains to realize the potential of renewable diesel production, especially regarding process integration between the bioconversion step and the catalytic lipid conversion into diesel blendstock. Moreover, technoeconomic analyses have identified the need of product recovery due to intracellular accumulation, and the aerobic cultivation conditions during the bioconversion process among the primary cost drivers.[49, 50]

In this work, we report on bench-scale production of diesel blendstock using a biological-catalytic hybrid process by converting lignocellulosic-based sugars to lipid fuel precursors using the oleaginous yeast *R. toruloides* and upgrading them via a hydrotreating process (**Figure 1**). Specifically, we screened a total of 31 different oleaginous yeast strains on corn stover hydrolysate for lipid production capabilities. Three strains were selected and further characterized in terms of lipid profiling, including neutral and polar lipid classing, demonstrating the accumulation of neutral lipids, mainly triacylglycerols (TAGs), over the course of the cultivation on corn stover hydrolysate. Moreover, the detoxification capability of the selected oleaginous strains to inhibitory compounds present in lignocellulosic-based hydrolysate was evaluated using a mock hydrolysate, demonstrating their capability of reducing and oxidizing aldehydes, and converting aromatic compounds. Furthermore, *R. toruloides* DSM-4444 was the only strain capable of using four different aromatic compounds as a sole carbon source. Cells of *R. toruloides* DSM-4444 were employed in a cell lysis and extraction process to isolate the lipid fraction, which was subjected to catalytic conversion (consisting of hydrodeoxygenation (HDO) and hydroisomerization (HI)) leading to a product within the range for diesel fuel. To our knowledge, this is the first report describing an integrated process for the production of diesel blendstock from lignocellulosic-based sugars using a biological-catalytic hybrid process.

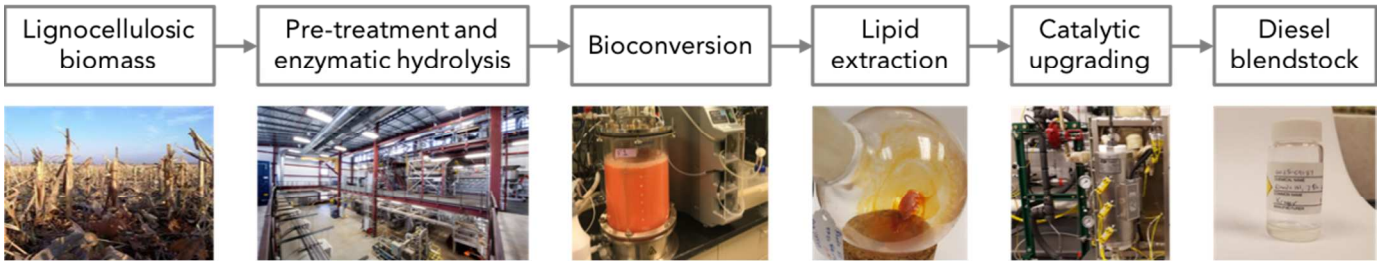

Figure 1. Process steps for the production of diesel blendstock from lignocellulosic biomass. In this work, bioconversion of lignocellulosic-based sugars to lipid fuel precursors is presented.

Results

Yeast screening on de-acetylated, dilute-acid pretreated, enzymatically hydrolyzed (DDAP-EH) corn stover hydrolysate

Small-scale strain screening is a useful strategy to evaluate a large number of strains in a systematic manner and to be able to quickly down-select the top performing candidates for a given application. However, the outcome of any screening procedure is highly dependent on the substrate of choice and cultivation conditions. This becomes especially critical when the final composition of the cultivation media triggers multiple synergistic effects regarding inhibition of metabolic events due to an increased pressure by compounds present in the growth medium. The importance of this was clearly exposed by Slininger *et al.*[51] in a screening to select good candidates for producing single cell oil from hydrolysates, when three of the top seven performing strains on synthetic medium reported by Dien and co-workers[52] did not grow on AFEX pretreated corn stover hydrolysate.[51, 52] Thus, in this study, the yeast screening to identify the strain with the best lipid production potential was performed using the same DDAP-EH corn stover hydrolysate to be used in the bioreactor evaluations. A total of 31 different yeast strains (listed in **Table S1**), belonging to seven different species, were screened in shake flasks on DDAP-EH corn stover hydrolysate diluted to an initial composition of 100 g L^{-1} monomeric sugars (glucose,

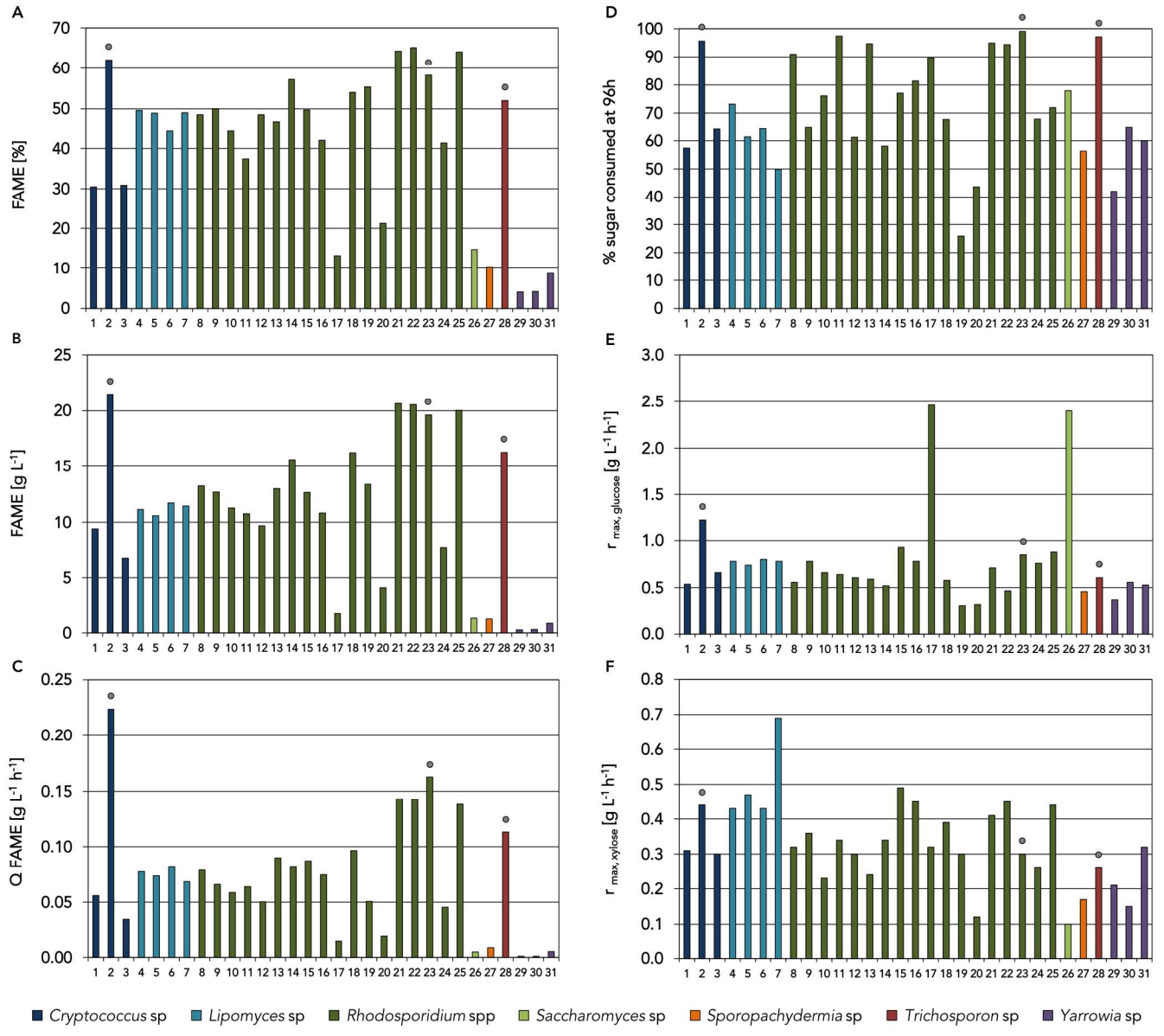

Figure 2. Lipid profiling measured as Fatty Acid Methyl Ester (FAME) determination, and sugar consumption from shake flask yeast screening on DDAP-EH corn stover hydrolysate. FAME content (%)(A), FAME titer (B), and FAME productivity (Q) (C), total sugar consumed at 96 h of cultivation (D), maximum glucose (E), xylose (F) consumption rates ($r_{max,\ sugar}$). The selected strains for further evaluation are highlighted with the symbol ●.

xylose, arabinose, and galactose) and supplemented with growth factors (yeast extract and peptone) (**Figure 2**).

Over the course of this study, some yeast species names have been updated based on ribosomal sequencing[53] and revisions on taxonomy (Dr. Kyria Boundy-Mills, personal communication). Since not all yeast culture collections have undergone a taxonomical revision, old species names have been maintained throughout the main text for clarity, and the updated names are included in **Table S1**.

All strains were inoculated at an optical density at 600 nm (OD_{600}) of 1.0 and monitored for growth and sugar consumption. Upon sugar depletion, a yeast biomass sample was taken, lyophilized, and its baseline lipid profiling was measured as fatty acid methyl ester (FAME). Candidate strains to be evaluated in fully controlled bioreactors were down-selected considering first FAME parameters, and then sugar consumption (**Figure 2**). To capture consumption of multiple sugars, the percentage of utilized sugars after 96 hours of cultivation was chosen as the criterion to compare the strains, as glucose and xylose depletion was observed for all strains between 72 and 192, and 120 and 216 hours of cultivation, respectively (data not shown). The strain *Cryptococcus curvatus* ATCC 20509 (strain #2 in **Figure 2**) consistently displayed the highest values, with a 62.12 % of FAME content (**Figure 2A**), up to 21.49 g L^{-1} final FAME titer (**Figure 2B**), and a FAME productivity of 0.22 g L^{-1} h^{-1} (**Figure 2C**). Thus, it was selected for further evaluation in fully controlled bioreactors. Among all tested *Rhodosporidium* strains included in this screening, four different *R. toruloides* strains (Y-27012, Y-27013, DSM-4444, and DSM-70398 – strains #21, #22, #23, and #25, respectively in **Figure 2)** were the best performers. Since they displayed similar values of FAME parameters, sugar consumption was also taken into consideration to down-select among those *R. toruloides* strains. After 96 h of cultivation, up to 99% of total sugars were consumed by the DSM-4444 strain, whereas less than 95% was consumed by the Y-27012 and Y-27013 strains. In the case of the DSM-70398 strain, less than 72% of total sugar was consumed after 96 h of cultivation (**Figure 2D**). Given the differences in sugar consumption rates, the DSM-4444 strain was selected as the candidate among the *Rhodosporidium* strains tested. In addition, *Trichosporon guehoae* UCDFST 60-59 strain (strain #28 in **Figure 2**) was also selected to be further evaluated in fully controlled bioreactors. This strain displayed a lower level of FAME content (51.97%) compared to the selected *C. curvatus* and *R. toruloides* strains, but similar to the *Lipomyces starkeyi* strains included in this screening (strains from #4 to #7 in **Figure 2A**). The UCDFST 60-59 strain was selected over *Lipomyces* strains, due to higher values of FAME titer (**Figure 2B**), FAME productivity (**Figure 2C**), and total sugar consumption after 96 h of cultivation relative to *Lipomyces* strains (**Figure 2D**). Regarding sugar consumption, most of the strains included in the screening displayed a maximum glucose consumption rate between 0.5 and 1 g L^{-1} h^{-1}, and only 3 strains exhibit values higher than 1 g L^{-1} h^{-1}: *C. curvatus* ATCC 20509 (1.23 g L^{-1} h^{-1}), *R. sphaerocarpum* UCDFST 68-43 (2.46 g L^{-1} h^{-1}), and the *Saccharomyces cerevisiae* strain D5A (2.40 g L^{-1} h^{-1}) (strains #2, #17, and #26, respectively in **Figure 2E**). Regarding maximum xylose consumption rate, all tested strains exhibit values below 0.5 g L^{-1} h^{-1}, except *L. starkeyi* UCSFST 78-23, which displayed the highest maximum xylose consumption rate of nearly 0.7 g L^{-1} h^{-1} (strain #7 in **Figure 2F**).

Selection of promising strains is highly dependent on the initial candidate strains under evaluation and the experimental conditions, especially when different lignocellulosic hydrolysates are used. Thus, comparison of screening processes in reported literature is quite challenging. For example, Slininger and coworkers evaluated 38 strains in the sequential screening on AFEX corn stover hydrolysate, and AFEX switchgrass hydrolysate using 96-well plates. The top performing strains, which were further evaluated in shake flask cultures using a two-stage lipid production strategy, were a *R. toruloides* strain and two *Lipomyces sp.* strains.[51] In the present work, *R. toruloides* strains were also identified as top candidates, but the tested *Lipomyces* strains were not ranked as the top performing strains because of low FAME accumulation, and thus not considered for further evaluation in fully controlled bioreactors. Instead, a *C. curvatus* strain and a *T. guehoae* strain were identified as top candidates. This example also clearly illustrates the importance of defining the screening conditions as analogous as possible to the application conditions, especially when complex substrates such as lignocellulosic-based feedstocks are being utilized.

Bioreactor cultivations on DDAP-EH

As shake flask screenings represent a fast and simple approach to obtain essential information, the larger, homogeneous volume when using a fully controlled bioreactor enables a more complete lipid analysis in a time-course fashion. Cultivations using the three strains selected for further evaluation (*C. curvatus* ATCC 20509, *R. toruloides* DSM-4444, and *T. guehoae* UCDFST 60-59) were thus performed in a 0.5 L controlled bioreactor on DDAPH-EH corn stover hydrolysate diluted to an initial composition of 100 g L^{-1} monomeric sugars (glucose, xylose, arabinose, and galactose) (**Table 1**). Seed cultures propagated for 24 hours on Yeast Nitrogen Base (YNB) medium supplemented with 50 g L^{-1} glucose and N-rich media components were used to inoculate the bioreactors at an OD_{600} of 1.0. In addition to growth and sugar consumption monitoring, cultures were sampled every 24 hours for FAME, free fatty acids, neutral lipids, and polar lipids analysis.

Table 1. Initial monomeric sugar concentrations in DDAP-EH corn stover hydrolysate and mock hydrolysate used in this study

Concentration	Glucose	Xylose	Arabinose	Galactose
g L^{-1}	58.17	34.63	5.11	2.09

C. curvatus ATCC 20509 displayed a sequential sugar consumption pattern where glucose was fully consumed

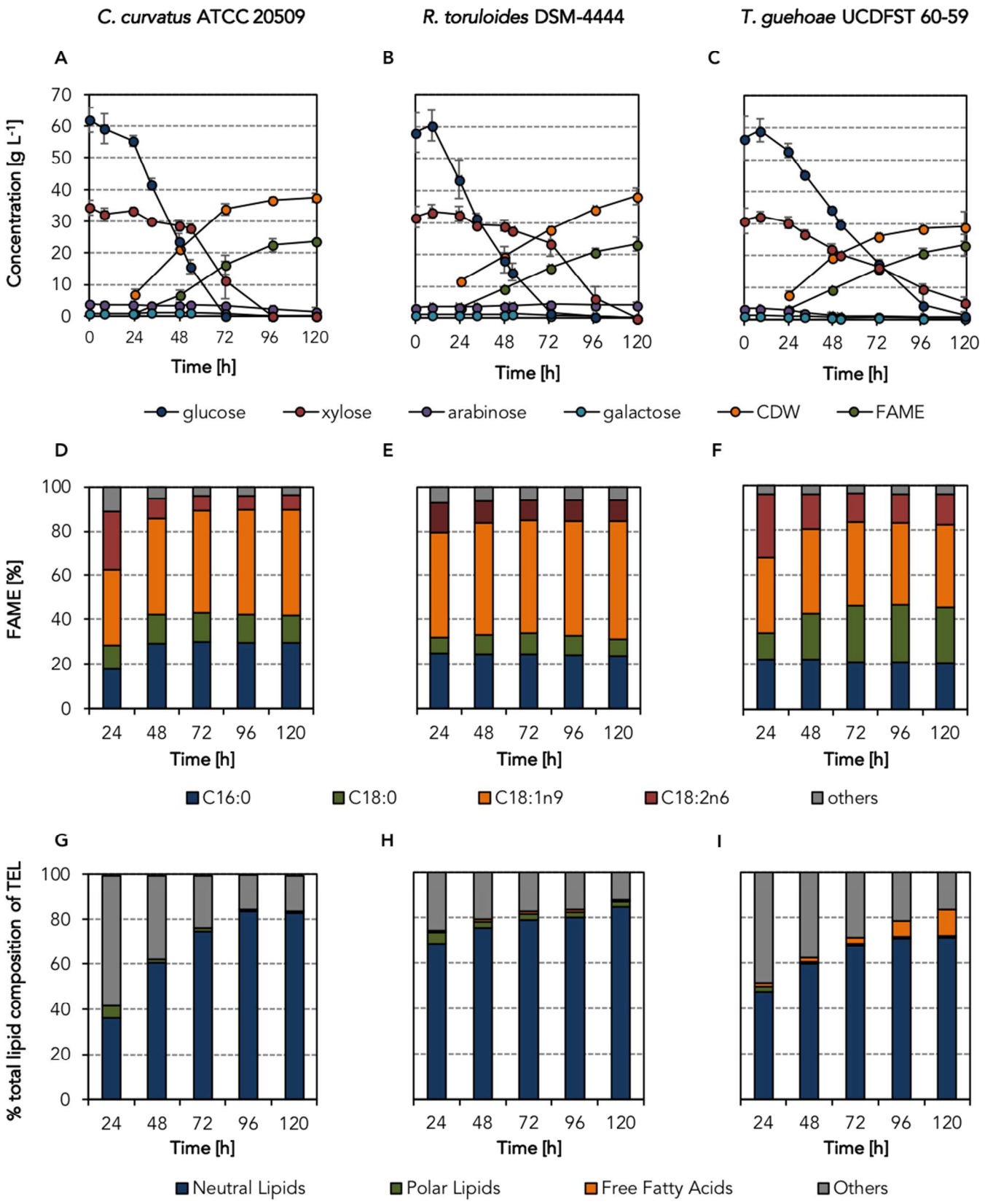

Figure 3. Bioreactor cultivations on DDAP-EH corn stover hydrolysate for *C. curvatus* ATCC 20509 (left column), *R. toruloides* DSM-4444 (middle column), and *T. guehoae* UCDFST 60-59 (right column) strains. Cultivation performance (A-C), FAME profiling (D-F), total lipid composition of total extractable lipids (G-I). Abbreviations: CDW: cell dry weight, FAME: fatty acid methyl ester, TEL: total extractable lipids

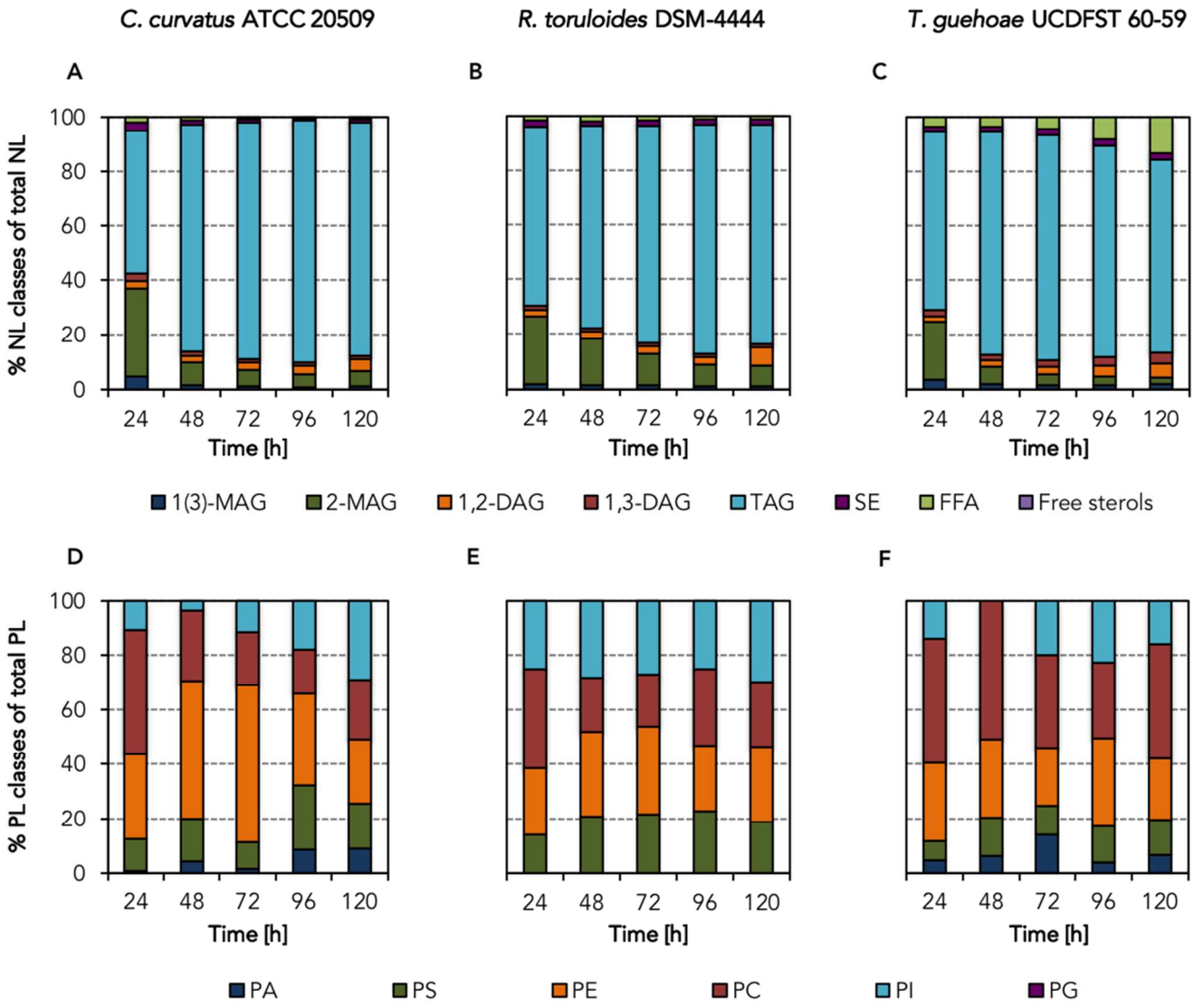

Figure 4. Bioreactor cultivations on DDAP-EH corn stover hydrolysate for *C. curvatus* ATCC 20509 (left column), *R. toruloides* DSM-4444 (middle column), and *T. guehoae* UCDFST 60-59 (right column) strains. Neutral lipids classing (A-C), and polar lipids classing (D-F). Abbreviations: NL: neutral lipids, PL: polar lipids, MAG: monoacylglycerol, DAG: diacylglycerol, TAG: triacylglycerol, SE: steryl ester, FFA: free fatty acid, PA: phosphatidic acid, PS: phosphatidylserine, PE: phosphatidylethanolamine, PC: phosphatidylcholine, PI: phosphatidylinositol, and PG: phosphatidylglycerol.

within 72 h, and clear xylose consumption was only observed when glucose levels were below 20 g L^{-1}. At the end of the cultivation, the FAME content of the *C. curvatus* strain was 63.1%, and up to 21.4 g L^{-1} FAME was obtained, representing a FAME yield of 0.24 g g^{-1} consumed sugars and overall FAME productivity of 0.22 g L^{-1} h^{-1} (**Figure 3A, Table 2**). Also, sequential sugar consumption was observed with *R. toruloides* DSM-4444. In this case, however, the glucose and xylose consumption rate were slower compared to the *C. curvatus* strain. As a consequence, the arabinose present in the cultivation media was not consumed after 120 h of cultivations. At the end of the cultivation, a slightly lower overall FAME productivity, and FAME content, 0.17 g L^{-1} h^{-1} and 60.8%, respectively, were observed. The final obtained FAME titer was 23.3 g L^{-1}, representing a FAME yield of 0.24 g g^{-1} consumed sugars (**Figure 3B, Table 2**). Differences in terms of sugar consumption were observed with the *T. guehoae* UCDFST 60-59 strain, where glucose and xylose, in addition to the minor sugars arabinose and galactose were co-consumed. Despite this pattern, glucose and xylose were not depleted after 120 h of cultivation, as all sugar consumption rates were slower than the ones observed with the *C. curvatus* and *R. toruloides* strains. At the end of the cultivation, a final FAME titer of 14.2 g L^{-1} was obtained, representing a FAME yield of 0.16 g g^{-1} consumed sugars. A significantly lower overall FAME productivity, 0.12 g L^{-1} h^{-1}, was obtained with *T. guehoae* compared to *C. curvatus*. Also, the final FAME content was significantly lower, 48.3 %, compared to that obtained with the other strains (**Figure 3C, Table 2**).

The strain *C. curvatus* ATCC 20509 has previously been evaluated on other lignocellulosic-based feedstocks. A higher yield was obtained but a lower lipid content was

Table 2. Cultivation performance parameters on DDAP-EH corn stover hydrolysate

Strain	% FAME	FAME [g L^{-1}]	Q FAME [g L^{-1} h^{-1}]	Y FAME [g g^{-1}]	Y biomass [g g^{-1}]
C. curvatus ATCC 20509	63.1 ± 3.7	21.4 ± 3.6	0.22 ± 0.03	0.24 ± 0.03	0.37 ± 0.03
R. toruloides DSM-4444	60.8 ± 1.1	23.3 ± 1.8	0.17 ± 0.04	0.24 ± 0.05	0.39 ± 0.08
T. guehoae UCDFST 60-59	48.3 ± 4.0	14.2 ± 3.3	0.12 ± 0.03	0.16 ± 0.05	0.33 ± 0.08

achieved when the performance of this strain was evaluated on sorghum stalk (0.29 g g^{-1} sugar and 60%, respectively) and switchgrass hydrolysate (0.27 g g^{-1} sugar and 58%, respectively) compared to the results obtained in the present study.[54] A much lower lipid performance was obtained with this strain when using dilute acid pretreated wheat straw hydrolysate. In this case, a lower FAME productivity (0.03 g L^{-1} h^{-1}), also coupled to a lower FAME content (33.5%) and yield (0.17 g g^{-1} sugar), demonstrating the presence of a higher level of inhibitors in this substrate.[55] Other *Cryptococcus* species have been also tested in other lignocellulosic-based feedstocks, such as corncob hydrolysates. In this case, and although a similar lipid content was obtained, much lower productivities and final titers were achieved, even when using fed-batch strategies.[56, 57] Overall, the results obtained with the *C. curvatus* strain on DDAP-EH corn stover hydrolysate positions the performance reported in this work among the best reported on lignocellulosic feedstocks. In the case of *R. toruloides*, different feeding strategies have been reported to improve the cultivation performance. The strain DSM-4444 was tested using the C6 fraction of corn stover hydrolysate, and compared to batch conditions, an increase of 43% in FAME productivity and 53% in yield was reported when the residual level of glucose was maintained at 10 g L^{-1} over the course of the cultivation.[58] The best performance to date on lignocellulosic-based hydrolysates has been reported with the *R. toruloides* Y4 strain, where up to 39.6 g L^{-1} of lipid titer and a productivity of 0.33 g L^{-1} h^{-1} was achieved under fed-batch conditions using concentrated Jerusalem artichoke hydrolysate.[59] Other oleaginous yeast have been tested on toxic hydrolysates or challenging conditions. For example, *L. starkeyi* performance was evaluated on thermochemical pretreated birch hydrolysate using a pH regulated fed-batch cultivation. In this case, acetic acid was co-consumed with xylose, and a final lipid titer of 8 g L^{-1} (representing a lipid yield of 0.1 g g^{-1}) coupled with a 51.3% lipid content was obtained.[60] Up to 5.78 g L^{-1} FAME were obtained when *Trichosporon cutaneum* was evaluated on corn stover at 20% solids.[61] Taken together, the obtained bioreactor results confirm that the screening conditions were optimal to identify the best lipid producing strains, as the results obtained for the three strains during the screening on shake flasks correlate well with the results obtained using fully controlled bioreactors.

Daily sampling, including yeast biomass, enabled FAME determination over the course of the bioreactor cultivations. FAME profiles for the three evaluated strains consisted essentially of the saturated palmitic (C16:0) and stearic (C18:0) acids, and the unsaturated oleic (C18:1n9) and linoleic (C18:2n6) acids. In the case of the *C. curvatus* cultivation, where the main fatty acids were palmitic and oleic acid, an increase of palmitic acid between 24 and 48 hours was observed, and the same level was maintained during the remainder of the cultivation. For the C18 fatty acids, a tendency to gain saturation over time was detected by decreasing levels of linoleic over oleic acid (**Figure 3D**). The FAME profiles in the case of the *R. toruloides* were more stable over time than in the two other evaluated strains. In this case, however, the highest fraction corresponded to oleic acid, at the expense of palmitic and stearic acid content (**Figure 3E**). In the *T. guehoae* cultivation, palmitic acid levels remained at the same levels over the course of the cultivation. Also, similarly to the *C. curvatus* strain, *T. guehoae* tended to gain saturation over time for the C18 fatty acids, where stearic and oleic acid content increased, and linoleic acid decreased between the 24 and 48 hours sampling point (**Figure 3F**). The presence of unsaturated linoleic acid in the FAME profile of all three oleaginous strains suggests the participation of at least two independent desaturase enzymes (Δ-9 fatty acid desaturase and Δ-12). Corresponding to the linoleic acid content in *C. curvatus* and *T. guehoae,* both Δ-9 and Δ-12 desaturase appeared to be more active in early exponential growth, and towards stationary phase of *T. guehoae* Δ-9 desaturase activity dropped resulting in less oleic and more saturated species. An increase in saturation of lipids with culture age has been previously observed in *Y. lipolytica* and other microorganisms.[62, 63]

In addition to the FAME profiles, total lipid composition (as a percentage of the total extractable lipids) was also analyzed over the course of the yeast cultivations. Since acid catalyzed FAME can be produced from the acyl chains of neutral lipids, polar lipids, and free fatty acids, it is important to understand the lipid source, not only because the backbone carbon waste from each lipid class is not equivalent, but heteroatoms such as phosphorus from the polar lipid class can be toxic to chemical catalysts. In the case of *C. curvatus*, free fatty acid levels remained minimal and stable over time, whereas neutral lipids increased during 96 h of cultivation and plateaued in the last sampling time point (120 h). An inverse tendency was observed in the case of polar lipids, with levels reduced after 48 h and remaining constant for the subsequent duration of the cultivation (**Figure 3G**). In the case of the *R. toruloides* strain, the neutral lipid fraction increased monotonically over the course of the cultivation, but the

overall increment was relatively lower, since the initial time point had a higher content than the other evaluated strains. Similar to *C. curvatus*, polar lipid levels of *R. toruloides* were reduced after 48 h, and remained at similar levels for the rest of the cultivation. Also, in this case, free fatty acid levels remained minimal and stable over time (**Figure 3H**). Additionally, like *C. curvatus*, the content of neutral lipids in the *T. guehoae* strain increased monotonically during the first 96 h of cultivation, and then plateaued in the last sampling time point (120 h), whereas the polar lipid fraction remained relatively stable over time. The main difference between *T. guehoae* and the other tested strains is the presence of a higher fraction of free fatty acids, which increased over the course of the cultivation (**Figure 3I**). This initial relative increase in polar lipid concentration in all strains likely accounts for the role that phosphatidic acid (PA) has on both neutral and polar lipid biosynthesis in the exponential growth phase wherein polar lipid synthesis is activated to contribute to cell membrane phospholipids. Simultaneously, PA also acts as an acyl-donor at this growth phase to assist in the formation of TAG. However, similarly with other oleaginous yeasts,[64] TAG synthesis increases through a neutral lipid pathway, thus increasing total neutral lipids over the cultivation time. Finally, the accumulation of free fatty acids of the *T. guehoae* strain over the harvest time indicates increased lipase activity of the organism compared to *C. curvatus* and *R. toruloides*.

Neutral and polar lipid classing was also performed in a time-resolved fashion. The *C. curvatus* strain displayed increasing levels of TAG over time between 24 and 48 hours and remained at more stable levels over time as the main neutral lipid class. This was coupled to a net decrease level of monoacylglycerols (1(3)-MAG, and 2-MAG), whereas the diacylglycerols (1,2-DAG and 1,3-DAG) levels remained essentially stable. Steryl ester and free fatty acid levels remained minimal and stable over the course of the cultivation (**Figure 4A**). In the case of the *R. toruloides* strain, TAG was also the main neutral lipid class, which increased over the first 72 h and maintained these levels until the end of the cultivation. This was combined with decreasing levels of 2-MAG over time, which plateaued in the last sampling point (120 h), whereas 1(3)-MAG and diacylglycerol levels remained stable over the course of the cultivation. Similarly to *C. curvatus*, steryl ester and free fatty acid levels remained minimal and stable over time for the *R. toruloides* strain (**Figure 4B**). The presence and subsequent decrease of MAG with the accumulation of TAG over the harvest time suggests the incorporation of MAG, either directly or indirectly, to TAG. To date, acyl-CoA:monoacylglycerol acyltransferases have not been described for yeast, although this re-esterification of MAG to DAG is an important step in plant and mammalian lipid metabolism.[65] MAG species comprising the neutral lipid pathway for TAG accumulation in these yeast strains warrants future study. As observed with the other two strains, TAG was also the main neutral lipid class in the *T. guehoae* strain cultivation. In addition, a similar trend as for the *C. curvatus* strain was observed, where increasing TAG levels were observed between 24 and 48 hours and remained at more stable levels during the course of the cultivation. This was coupled to an inverse trend of MAG levels. In addition, and a slight increase of DAG levels were observed over time. Similarly, with the other two strains, steryl ester levels remained minimal and stable over time, but contrary to the other strains, the *T. guehoae* strain clearly exhibits an increase of free fatty acid levels over the course of the cultivation (**Figure 4C**). The decrease in TAG with a corresponding increase in DAG and free fatty acids, indicates breakdown of TAG into its components and further strengthens the hypothesis of increased lipase activity towards the 120 h time point. Of the neutral lipid classing, TAG was further speciated to offer insight above that of FAME profiling (as shown in **Figure S2**).

Regarding polar lipid classing, phosphatidylethanolamine (PE) and phosphatidylcholine (PC) were initially the main classes observed in the *C. curvatus* strain. The initial levels of PC decreased at 48 h and remained stable over time, and the level of PE peaked at the 72 hours sampling point. This was coupled to an increase of phosphatidylinositol (PI) levels at the end of the cultivation, and a relatively stable level of PA (**Figure 4D**). Along with the absence of phosphatidylglycerol (PG), these observations follow the cytidine diphosphate diacylglcerol (CDP-DAG) pathway for yeast, where PA is converted to either PI or phosphatidylserine (PS), PS continues to be converted to PE, and finally to PC.[64, 66] With this in mind, the *C. curvatus* strain initially partitioned the CDP-DAG pathway towards PC, but towards the end point of the cultivation, PI additionally accumulates as well. For *R. toruloides*, there was only the presence of four different polar lipid classes (PE, PS, PI, and PC) at roughly similar levels, which remained stable over the course of the cultivation indicating that PA was being utilized rapidly (**Figure 4E**). Similarly to *R. toruloides*, levels of PA, PE, PS, PI, and PC remained relatively stable over the course of cultivation with the *T. guehoae* strain (**Figure 4F**). Similarly to TAG, polar lipid classes were also speciated, as reported in **Figure S3.**

The top three yeast strains selected for further evaluation exhibit similar lipid growth profiles. A thorough characterization of lipid production and sugar utilization over the course of cultivation shows that at 96 h, the majority of sugars were consumed for all three strains and lipid profiles were mature and did not alter with additional fermentation time (FAME, neutral, polar lipids), with the exception of lipase activity from *T. guehoae*. In addition to FAME profiling, lipid class profiling was necessary to determine fatty acid origin, and therefore, to ensure carbon to fuel precursor efficiency. Based on ideal fuel precursor (lipid class and fatty acid profile), as well as production parameters (yield, productivity, and titer), the optimal strains for further conversion would be *R. toruloides* and *C. curvatus*.

Cultivations on mock hydrolysate

When lignocellulosic biomass is hydrolyzed to release monomeric sugars, degradation compounds are also formed. Aldehydes, such as 5-(hydroxymethyl)furfural (5-HMF) and furfural, are generated via sugar dehydration. In addition, aromatic compounds are released as result of lignin degradation. The presence of these compounds in the resulting hydrolysate can negatively impact the metabolism of microorganisms. To evaluate potential toxicity tolerance mechanisms, the selected strains were inoculated into a synthetic hydrolysate containing 100 g L^{-1} of total initial sugars (at the same ratio of glucose, xylose, arabinose, and galactose present in DDAP-EH corn stover hydrolysate) (**Table 1**), in addition to 8 different inhibitory compounds (5-HMF, 4-hydroxybenzaldehyde, vanillic acid, caffeic acid, syringic acid, vanillin, *p*-coumaric acid, and ferulic acid).

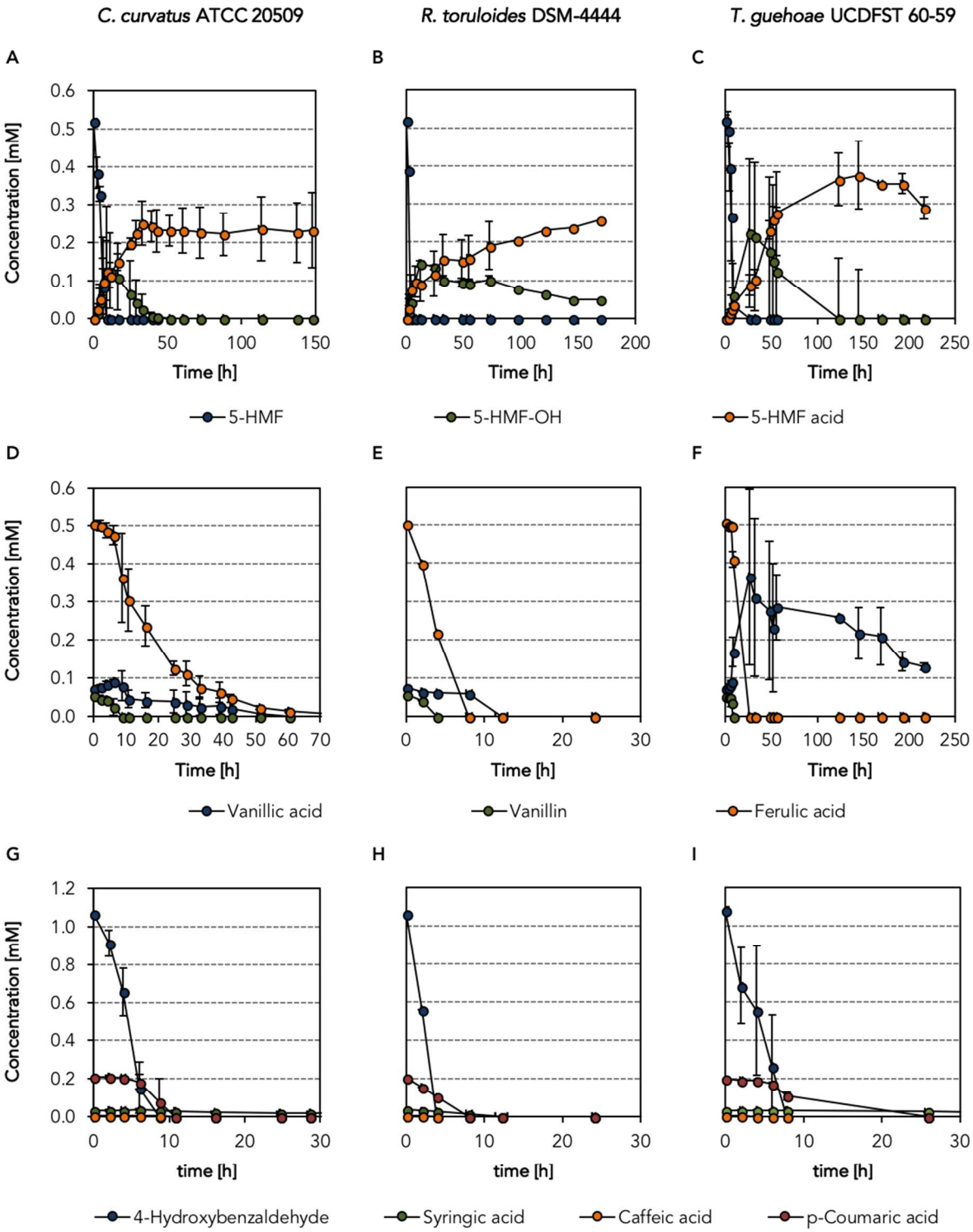

Figure 5. Shake flask cultivations on mock hydrolysate for *C. curvatus* ATCC 20509 (left column), *R. toruloides* DSM-4444 (middle column), and *T. guehoae* UCDFST 60-59 (right column) strains. For clarity, profiles of lignocellulosic degradation compounds are presented in different graphs.

To extend the conversion time profiles and asses conversion, concentrations of inhibitory compounds were doubled based of the ones present in DDAP-EH corn stover hydrolysate.

Strains were inoculated at the same OD_{600} of 1.0, and samples were taken over time for sugar assimilation and inhibitory compound conversion until the sugars were depleted (sugar profiles are summarized in **Figure S4**). In the case of the *C. curvatus* strain, 5-HMF was completely converted within 9 hours of cultivation. Although 5-HMF was simultaneously converted to 5-(hydroxymethyl)furfural alcohol (5-HMF alcohol) and 5-(hydroxymethyl)furfural acid (5-HMF acid), different trends where observed for these two compounds when 5-HMF was fully depleted. Specifically, the maximum 5-HMF alcohol concentration was observed when 5-HMF was fully depleted, and the 5-HMF acid level continued increasing due to a molar conversion of 5-HMF alcohol to 5-HMF acid. The level of 5-HMF acid remained stable for the rest of the cultivation (**Figure 5A**). Like 5-HMF, vanillin was also assimilated within 8 hours of cultivation. In the case of the aromatic acids, vanillic acid and ferulic acid were completely depleted after 60 and 87 hours of cultivation, respectively (**Figure 5D**). Similarly, decreasing profiles were observed for all the other inhibitors. Namely, 4-hydroxybenzaldehyde, caffeic, and *p*-coumaric acid were converted within the first 16 hours of cultivation, and up to 133 hours were required to have full conversion of syringic acid in the *C. curvatus* strain cultivation (**Figure 5G**).

Some important differences were observed with the *R. toruloides* strain. Initially, 5-HMF was also converted simultaneously to 5-HMF alcohol and 5-HMF acid within the first 4 hours of cultivation. Further conversion of 5-HMF alcohol to 5-HMF acid was slower than in *C. curvatus*, as 5-HMF alcohol was still detected when sugars were fully depleted (**Figure 5B**).

Overall, the *R. toruloides* strain showed a higher capability of inhibitor conversion, as all other degradation compounds initially present in mock hydrolysate were completely converted within 12 hours of cultivation (**Figure 5E and H**). In the case of *T. guehoae*, 5-HMF was also simultaneously converted to 5-HMF alcohol and 5-HMF acid, in this case within 24 hours of cultivation. Similarly to the *C. curvatus* strain cultivation, 5-HMF alcohol was completely depleted when sugars were still present in the media (**Figure 5C**). In addition, a unique catabolic pathway was observed for this strain, as ferulic acid was converted first to vanillic acid within 24 hours, and then re-assimilated over the course of the cultivation (**Figure 5F**). Conversion of ferulic acid to vanillic acid through the β-oxidation pathway has been extensively reported in bacteria, including among them, the oleaginous bacteria *Rhodocous opacus*.[67] In the case of fungal systems, this conversion is described via propenoic chain degradation instead,[68] and to the best of our knowledge the conversion of ferulic to vanillic acid is first shown for the oleaginous yeast *T. guehoae* in the present study. The accumulation of vanillic acid, however, would indicate a low efficiency on further assimilation. On the other hand, *p*-coumaric acid was also fully converted within 24 hours, and it required up to 8 hours in the case of 4-hydroxybenzaldehyde. Caffeic acid was assimilated within 6 hours, whereas it required up to 169 hours of cultivation in the case of syringic acid (**Figure 5I**).

Due to similar chemical structures, detoxification mechanisms and assimilation pathways for 5-HMF and furfural are often equivalent, and previously reported evidence can help to elucidate the different assimilation pathways in other microorganisms. Exclusive conversion of furfural to 2-furoic acid, not to furfuryl alcohol, has been observed in the case of *P. putida* and *E. coli,*[69] whereas the degradation of 5-HMF via HMF acid and its further metabolism through the furfural assimilation route has been described in the bacterium *Cupriavidus basilensis.*[70] Similarly to what was observed for 5-HMF with all the evaluated strains, simultaneous conversion of 5-HMF and furfural to its corresponding acids and alcohols has been also observed with the fungi *Amorphotheca resinae* ZN1[71] and *Pleurotus ostreatus*.[72] In the case of *T. fermentans*, another oleaginous yeast, this organism initially reduces furfural to furfuryl alcohol during the lag phase, and then the concentration of furfuryl alcohol decreases while the concentration of furoic acid increases,[73] as observed here with all tested strains. This capability to reduce and oxidize furanic compounds under aerobic conditions would suggest a versatility of detoxification mechanisms, contrary to *S. cerevisiae*, in which furfural was reported to be exclusively converted to furoic acid during respiratory growth, and to furfuryl alcohol during anaerobic growth.[74] Similarly to *Pleurotus ostreatus,*[72] *Cupriavidus basilensis,*[75] and an engineered *P. putida* strain,[76] the tested strains showed the potential ability to assimilate furaldehyde compounds to enhance carbon conversion of lignocellulosic streams.

Cultivations on mineral medium with aromatic compounds as carbon source

Valorization of lignin-rich streams in a biorefinery will be essential for the overall economic viability of lignocellulose conversion.[50] To assess if oleaginous yeasts could potentially be used as organisms for microbial lignin valorization strategies,[77] ferulic acid, vanillic acid, *p*-coumaric acid, and 4-hydroxybenzoic acid were tested as a sole carbon source. They have previously been identified in the lignin-enriched streams obtained from corn stover subjected to an alkaline pretreatment, and are often used as model aromatic lignin compounds.[78] In addition, the ability to metabolize aromatic compounds also present in lignocellulosic-based hydrolysates would contribute to an improvement of total carbon conversion. The selected strains, *C. curvatus* ATCC 20509, *R. toruloides* DSM-4444, and *T. guehoae* UCDFST 60-59, were inoculated into YNB medium supplemented with *p*-coumaric acid, ferulic acid, vanillic acid, or 4-hydroxybenzoic acid. All strains were inoculated at the same OD_{600}, and samples were taken over time to monitor potential aromatic

compound assimilation (OD_{600} profiles are summarized in **Figure S5**).

Only *R. toruloides* was capable of using all tested lignin-derived acids. It was able to consume 4-hydroxybenozoic acid and vanillic acid within 72 and 96 hours, respectively. Conversely, full consumption of ferulic and *p*-coumaric acid by *R. toruloides* was only observed after 120 and 168 hours of cultivation, respectively. These results are in agreement with Yaegashi and co-workers, who also recently reported the capability of another *R. toruloides* strain (IFO 0880) of utilizing the same lignin-derived compounds as a sole carbon source.[27] In the case of *C. curvatus* and *T. guehoae* strains, they were only capable of using 4-hydroxybenzoic acid as a sole carbon source, as even after one week of cultivation, no consumption of *p*-coumaric, ferulic, or vanillic acid was observed (**Figure 6**). The consumption profile of 4-hydroxybenzoic acid was different for each strain. Whereas the *R. toruloides* strain fully consumed the aromatic compound within 72 hours, up to 168 hours were required for the other two strains. Moreover, although *C. curvatus* followed a similar consumption profile as *R. toruloides* during the first 48 hours, its consumption slowed considerably for the remainder of the cultivation. In the case of the *T. guehoae* strain, the consumption profile of 4-hydroxybenzoic acid was drastically lower over the course of the whole cultivation (**Figure 6**). Yaguchi *et al*. recently demonstrated not only the capability of *C. curvatus* 20509 to grow on different lignin-derived aromatic compounds, including 4-hydroxybenzoic acid, but also to remain oleaginous during the cultivation, showing its potential as an organism of choice for the production of biofuels from depolymerized lignin.[79] Moreover, the capability of utilizing the tested compounds as a sole carbon source has also been reported for other oleaginous yeast and bacteria.[80, 81] Assimilation of other aromatic compounds via the central intermediates catechol, and protocatechuate via the β-ketoadipate pathway have been demonstrated for different oleaginous yeast species including *Rhodotorula graminis*[82] and *Trichosporon cutaneum*,[83] and oleaginous bacteria such as *Rhodococcus jostii*.[84]

The use of lignin model compounds, including oligomers, polymers and lignin degradation products, represents a fundamental platform to elucidate the metabolism of aromatic compounds by oleaginous microorganisms. However, at the same time, the utilization of real lignin streams, as recently reported for extracted lignin from alkali pretreated corn stover using *Rhodotorula mucilaginosa, Rhodococcus opacus*, and *Rhodococcus jostii* strains,[78, 85-87] will help to assess the feasibility of using oleaginous microorganisms for the biological conversion of biomass-derived lignin to lipids in a more holistic biorefinery.

Lipid extraction

In the interest of demonstrating a fully integrated process, lipid extraction from mixed sugars- and hydrolysate-cultivated yeast was also explored. Harvested yeast cells were washed, lysed with aqueous acid, and extracted with hexane using the method developed by Kruger *et al*.[88] Briefly, the harvested cells were diluted to 8 wt% yeast solids in water and lysed at 170°C for 60 min with 1 wt% H_2SO_4. Following the acid treatment, the lysed cell slurries were extracted with an equal volume of hexane four sequential times, the hexane was evaporated, and the recovered lipids were analyzed for FAME content[89] and compared to the FAME content of the starting cell mass. As shown in **Figure 7**, greater than 90% of the lipids could be recovered from all of the strains by this protocol, whether the yeast was cultivated on mixed sugars or hydrolysate.

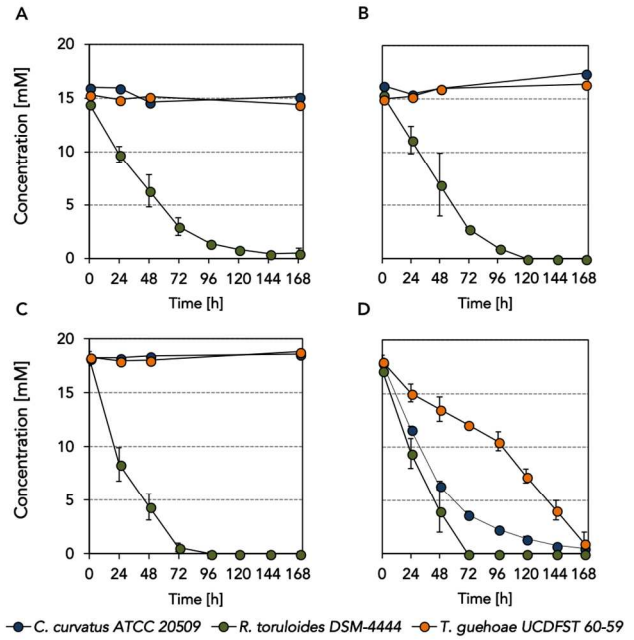

Figure 6. Shake flask cultivations on YNB media supplemented with *p*-coumaric acid (A), ferulic acid (B), vanillic acid (C), or 4-hydroxybenzoic acid (D) as a sole carbon source for *C. curvatus* ATCC 20509, *R. toruloides* DSM-4444, and *T. guehoae* UCDFST 60-59 strains.

Surprisingly, the extraction trend varied significantly across species and cultivation media. In mixed sugars media (**Figure 7**), *C. curvatus* lipids were readily extractable, with 93.7% recovered in the first extraction, and greater than 99% after the second extraction. In contrast, only 43.9% and 38.0% of the lipids from *R. toruloides* and *T. guehoae*, respectively, were recovered in the first extraction, and neither gave a recovery yield above 90% until the fourth extraction. When the cultivation medium was changed to biomass hydrolysate (**Figure 7B**), however, *C. curvatus* lipids became much less extractable, with only 42.7% recovered in the first extraction. Hydrolysate-cultivated *T. guehoae* also exhibited a low recovery yield of 55.5% in the first extraction, while *R. toruloides* exhibited an 83.3% recovery yield.

The reason for these differences is not well understood at this point, but may arise from the stress response of each strain —either the nutrient limitation required for lipid

accumulation or toxic components in the hydrolysate.[90-94] It is also possible that the superior ability of *R. toruloides* to utilize aromatic compounds in the hydrolysate, delayed its stress response and subsequent recalcitrance to lipid extraction. The observation that greater than 90% of the lipids could be recovered in all cases suggests that acid hydrolysis is effective across strains and cultivation media, but that different components in the post-lysis slurries may inhibit the hexane extraction. These differences underscore the importance of integrated studies of full biorefinery process flows, as changes in lipid extractability will affect the size and solvent consumption in the extraction unit operation. Further exploration of these effects is outside the scope of this study, but because of the superior performance of *R. toruloides* in hydrolysate (including a higher capability of inhibitor conversion), the ability of growth on four aromatic compounds as a sole carbon source, and the provision of genetic tools for metabolic engineering strategies, we elected to scale up this strain for conversion of the yeast lipids into diesel blendstock.

Lipid conversion into diesel blendstock

To generate sufficient lipid mass for hydroprocessing experiments, *R. toruloides* was cultivated in mixed sugars media. YNB medium supplemented with an initial composition of 100 g L^{-1} of total sugars (at the same ratio of glucose, xylose, arabinose, and galactose present in DDAP-EH corn stover hydrolysate) was used to perform a 10 L batch cultivation, which was carried out until sugar depletion. The broth was centrifuged, and the yeast pellet was washed with water and stored at -80°C until pretreatment and extraction.

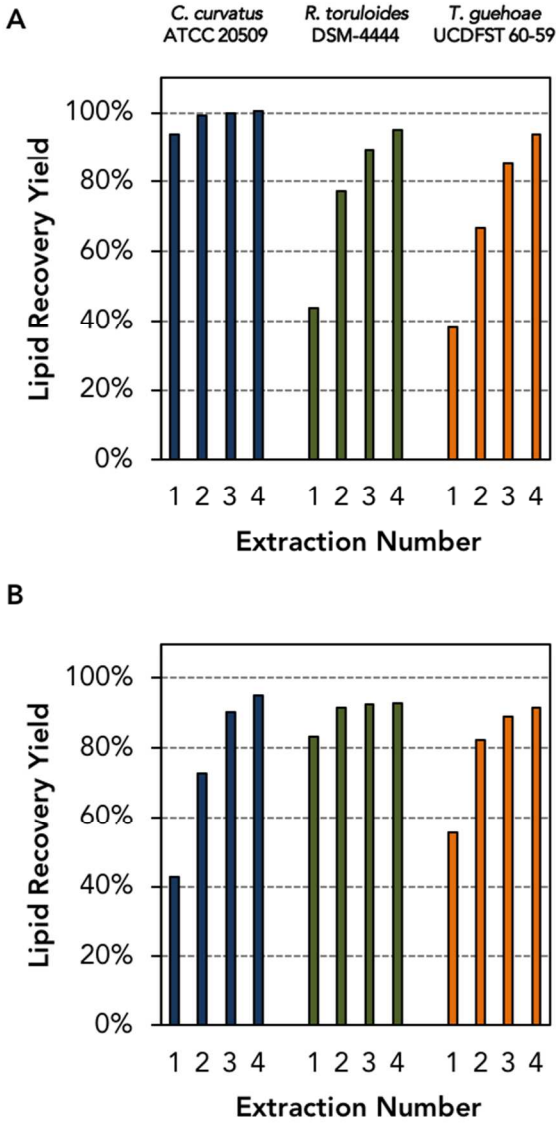

Figure 7. Lipid extraction yields from harvested oleaginous yeast grown in mixed sugars (A) and biomass hydrolysate (B).

Figure 8 shows the steps of the conversion process. Pretreatment was carried out in a Zipperclave reactor in batch mode at an initial concentration of yeast of *ca*. 8% wt, and 1% wt H_2SO_4 at 170°C for one hour. The resulting slurry was transferred to a round bottom flask, and hexane was added to the same initial yeast concentration (8% wt) to perform the lipid extraction step. The system was stirred overnight to facilitate the extraction to the hexane phase. Upon phase separation, the organic phase was transferred into a second round-bottom flask where hexane was evaporated under vacuum, yielding a semi-solid paste at room temperature (**Figure 8B**). The initial color of the lipid extract was orange due to an extraction of carotenoid compounds with the lipids. Although present in relatively

small amounts, removal of carotenoids prior to hydrotreating would be advantageous, as they represent a valuable coproduct,[95] and their presence increases the hydrogen consumption due to a high degree of unsaturation.

The lipid extract was dissolved in hexane to be pumped into the hydrotreating reactor (**Figure 8C**). The HDO reaction liquid-phase yields averaged 79.9% through 35 h time-on-stream (TOS). Online GC analysis showed that the reaction reached steady state after about 10 h TOS, after which CO and CO_2 production were around 0.05 and 0.02 g g^{-1} oil, respectively. Similarly, apparent hydrogen consumption averaged roughly 0.01 g H_2 g^{-1} oil (**Figure 9**).

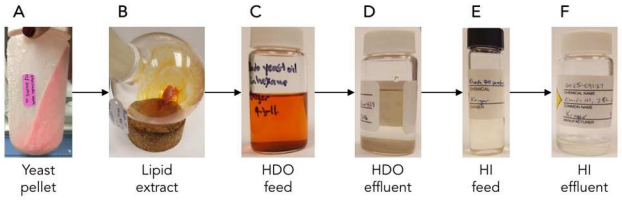

Figure 8. Pictures illustrating the process of lipid conversion into diesel blendstock.

The liquid phase (**Figure 8D**) contained C15-C18 *n*-alkanes, primarily C15 and C17, (two largest peaks in Figure S1A, respectively), indicating that the major pathways for oxygen removal were through decarbonylation and decarboxylation. This is consistent with previous research on lipid deoxygenation over Pd/C catalysts showing C_{n-1} normal alkanes as the primary products from C_n fatty acid chains.[96] Under similar conditions, an oleic acid control reaction without catalyst gave high conversion, but only partial deoxygenation and partial saturation of double bonds.[96] The liquid product also contained lighter and heavier alkanes from cracking and recombination reactions, respectively, which is likely due to the severe conditions of the HDO reactor. Fatty acids are increasingly prone to thermal cracking reactions above 300°C,[97, 98] and the high pressure may be favorable for oligomerization reactions of unsaturated compounds, which oligomers can then also subsequently crack to yield compounds in the C20-C35 range.

Upon separation of the organic phase and evaporation of the hexane solvent, this mixture of alkanes exhibited a cloud point near room temperature (22.6°C) (**Figure 8E**), but could be kept liquid for prolonged periods by immersing its container in warm water. This mixture of alkanes was hydroisomerized, giving a clear liquid product in 67.9% yield after 7.5 h time-on-stream (**Figure 8F**).

After isomerization, the liquid product initially exhibited a cloud point of 5.6°C, measured by differential scanning calorimetry, which is significantly decreased from the HDO product, reflecting the isomerization of paraffins into isoparaffins (**Figure 10A**), and the cracking of heavier components into diesel and naphtha range components (**Figure 10B** and **Figure S1**). However, the cloud point was higher than expected, and was likely due to the presence of a small fraction of heavy alkanes in the HDO product that were not converted in the HI step. These components formed wax crystals that could be easily filtered out with minimal yield losses by dissolving the HI product in hexane, holding the solution at -20°C and filtering while cold. After this cold filtration step, the cloud point was measured to be -14.5°C.

Simulated distillation of the HI product yielded the boiling curve where approximately 75% of the product was in the diesel range, using a cutoff temperature of 175°C to distinguish between gasoline and diesel fractions. Similarly, the T90 of the material was within the acceptable range (282-338°C) for No. 2 diesel fuel (**Figure 10C**).

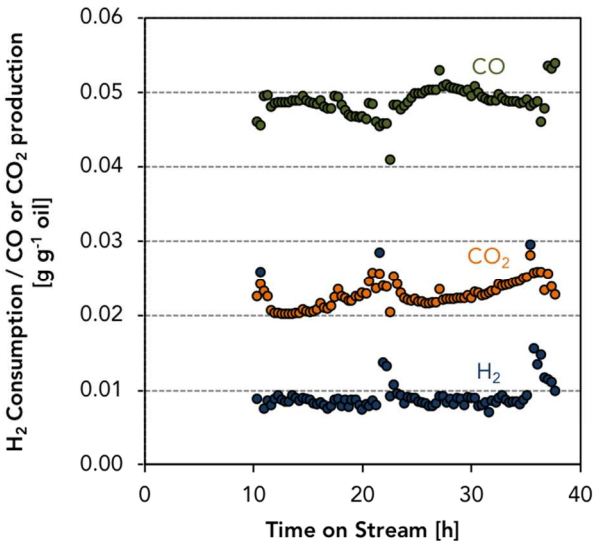

Figure 9. De-CO_x product formation and H_2 consumption during R. Toruloides oil deoxygenation. Reaction conditions: 450 °C, 1300 psig H_2, LHSV = 1 hr^{-1}.

The hydrotreating conditions were relatively harsh compared to what has been required for deoxygenation of lipid feedstocks in previously reported studies.[99] The conditions used in the present experiments were informed by our previous work with crude, hexane extracted algal lipids, which required high temperature and pressure to remove impurities, particularly nitrogen.[96] Since the nitrogen content of the yeast lipid extract was unknown,

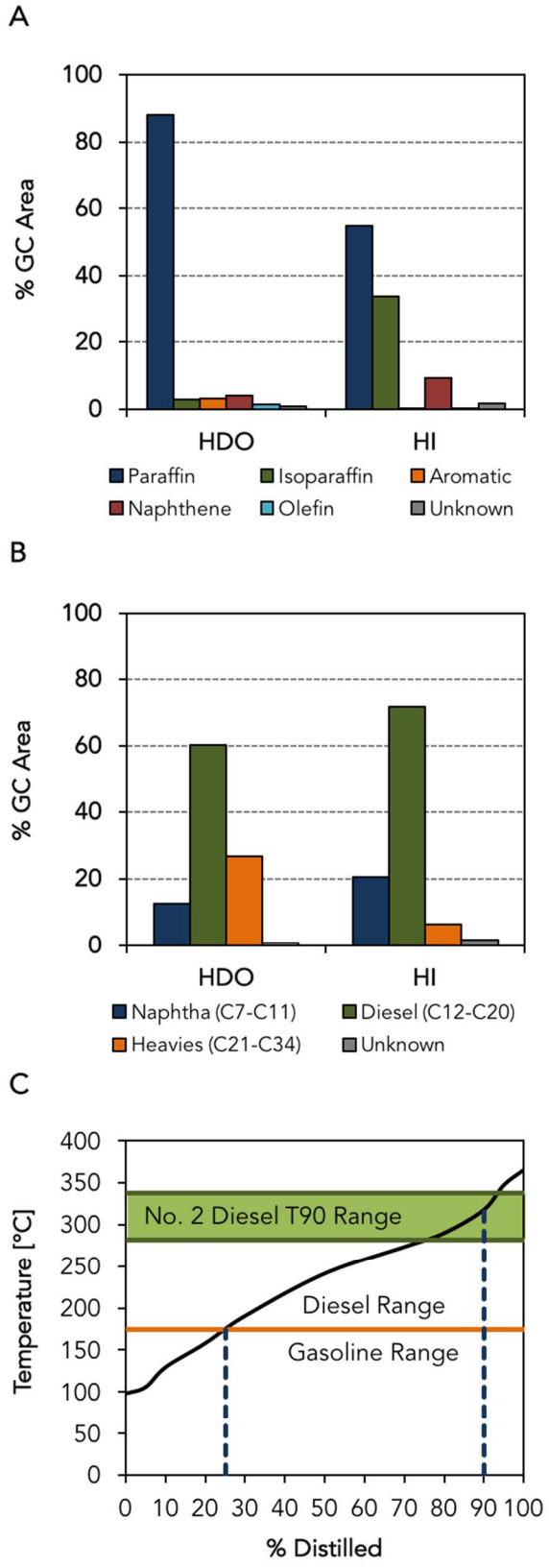

Figure 10. *R. toruloides* DSM-4444 strain lipid conversion. Hydrocarbon speciation (A), and hydrocarbon distribution according to molecular weight (B) of hydrodeoxygenation (HDO) and hydroisomerization (HI) liquid product characterization by GC/MS. Simulated distillation curve measured for deoxygenated, isomerized product (C).

conservative conditions were employed to ensure a successful conversion to diesel blendstock. Therefore, conditions could likely be improved if more detailed analysis of the yeast lipid extracts suggested low impurity levels. The origin of the heavy fraction is not well understood at this point, but may be partly due to recombination of thermal decomposition products.[100]

Discussion

In this work, we have demonstrated an integrated, bench-scale process for converting lignocellulosic sugars in an industrially-relevant hydrolysate stream to a fungible diesel blendstock by converting the sugars, both pentoses and hexoses, to a lipid fuel precursor in oleaginous yeast, lysing the yeast cells to recover the lipids via hexane extraction, deoxygenation of the crude recovered lipids over a Pd/C catalyst, and isomerizing the deoxygenated lipids over a Pt/SAPO-11 catalyst. Accordingly, this work demonstrates the relatively high technical readiness level of the combined biological-catalytic processing of the sugars-lipids-fuel approach to drop-in cellulosic biofuels. Previous economic analyses have shown that this approach is likely capable of producing biofuel with a minimum selling price in the range of $4-5/gallon of gasoline equivalent.[49, 88] Some of the main contributing factors to this selling price are the relatively expensive cultivation of the yeast due to strict aerobic requirements, the relatively low metabolic yield of sugars to lipids, the ongoing need for acid (and alkali for post-extraction neutralization) to lyse the cells, solvent losses in the extraction step, and capital costs for the hydroprocessing reactors due to the relatively severe conditions employed here. While the furthest downstream process expenses can likely be improved by judicious engineering (e.g., increasing lipid recovery yields by using a continuous countercurrent extraction column, decreasing solvent losses by using a multi-component extractant, and decreasing hydroprocessing severity by catalyst and process development), the mid- and upstream processes are likely to remain significant cost drivers due to the fundamental nature of lipids as an aerobic intracellular product. At production scale, microbial performance is often highly dependent on mass and heat transfer. High mixing times lead to gradients in temperature, pH, gradients in nutrients, substrates and gas, as well as the hydrostatic pressure in the bioreactor. These effects may become even more acute when the cellular pathway is oxygen dependent, as it is for lipid production.[101, 102] Moreover, the accumulation of lipids as an intracellular product introduces two key challenges: a significant fraction of sugars is converted to cell mass instead of fuel precursor, and the cells must be lysed to release and recover the lipids.

There are multiple scientific approaches to overcome these challenges. First, the use of a combined approach to screen for strains with high lipid production capabilities in a short period of time will continue to be essential to increase the size of the screening. Over the last years, researchers have used an initial qualitative assessment, such as thin layer chromatography[103] or Nile Red staining,[104] with a

quantitative determination of lipid production to identify superior candidate strains for the production of lipids. In addition, lipid accumulation can be promoted by bioprocessing optimization. The use of fed batch strategies can uncouple the growth phase and the lipid accumulation phase by having a substrate limited in nitrogen or other nutrient during the feeding period.[23] Second, the yeast may be engineered to secrete lipid fuel precursors, such as fatty alcohols[105] or aldehydes, despite the fact that metabolic engineering of non-model organisms has proven to be much more difficult. A stronger preference for non-homologous end-joining and low activity for integration via homologous recombination is presumably the cause, since many of the genetic tools rely on the high capacity of the microorganism to undergo homologous recombination (for a recent review see Shi and Zhao[106]). Third, the yeast may be triggered to autolyse instead of requiring an explicit set of unit operations for cell lysis. This activity has been observed in *S. cerevisiae* strains employed to enhance the flavor profile in sparkling wine,[107] but also facilitating the polyhydroxyalkanoate recovery in the bacterium *Pseudomonas putida*.[108] Fourth, the yeast may be cultivated as a biofilm instead of in a bioreactor to enhance gas transfer rates to the growing yeast in a less expensive manner than bubbling compressed air through a growth medium. This approach would also decrease the energy intensity of the harvesting step because the yeast could be scraped off the biofilm instead of being processed in a centrifuge. Fifth, the lipid fraction of yeast biomass which does not consist of lipid fuel precursors could be valorised by recovering coproducts (e.g., sterols, trehalose or carotenoid pigments).[109]

It is also worth noting that the relatively low metabolic yield of sugars to lipids is offset by the resemblance of lipids to a finished fuel. That is, the typical metabolic yield of sugars to lipids of 0.24 g lipid/g sugar combined with a theoretical lipid recovery yield of 100% and a theoretical deoxygenation/hydroisomerization efficiency of 85-90% (depending on the speciation of the fatty acid chains and the chemistry of oxygen removal as H_2O, CO, or CO_2) to give a theoretical sugar-to-fuel yield of roughly 0.2 g fuel/g sugar input. The high conversion efficiencies are possible because the lipids contain only ~10% oxygen. For comparison, ethanol can be produced at a theoretical metabolic yield of 0.51 g/g sugar (commercial plants using sugar cane can operate at roughly 90% of this value),[110, 111] but contains ~35% oxygen. Conversion of ethanol into hydrocarbon fuels frequently results in primarily gasoline-range mixtures,[112-114] although a few efforts have focused on producing diesel-range materials. In general, these approaches involve dehydration to ethylene and oligomerization to the appropriate carbon number range. The oligomerization of light olefins is typically able to generate 50-70% yield to diesel range hydrocarbons.[115-117] Assuming a 70% efficient ethylene oligomerization strategy to produce diesel-range carbon chains, the overall efficiency would be ~0.2 g diesel-range fuel/g sugar from ethanol. Thus, overall, the lipid pathway for cellulosic biofuels is in the range of alcohol-based pathways in terms of mass efficiencies, but further process development is necessary to improve the economics of the overall process.

Moreover, we have demonstrated, consistent with several previous studies, that oleaginous yeasts were not only able to metabolize several of the inhibitors present in lignocellulosic-based hydrolysates, but also to use aromatic compounds as a sole carbon source. However, there is a need of systematic studies to elucidate the aromatic catabolic pathways in these oleaginous yeasts as it has been conducted in aromatic degrading bacteria.[77, 118, 119] Also, improved genome and functional annotation would also allow a more comprehensive understanding of the multiple lignin degradation pathways in oleaginous yeast strains. Ultimately, in a broader context such as in biorefineries, polysaccharide and lignin valorization in parallel or simultaneously will be key to maximize the economic profitability of lignocellulosic biorefining.

Experimental

Material and Methods section can be found in Electronic Supplementary Information.

Conflict of interests

There are no conflicts to declare.

Acknowledgements

This work was authored by Alliance for Sustainable Energy, LLC, the manager and operator of the National Renewable Energy Laboratory for the U.S. Department of Energy (DOE) under Contract No. DE-AC36-08GO28308. Funding was provided by the DOE Energy Efficiency and Renewable Energy (EERE) Bioenergy Technologies Office (BETO). Dan Schell and the team at NREL's Biochemical Conversion Pilot Plant are gratefully acknowledged for providing DDAP-EH corn stover hydrolysate. We thank Earl Christensen for analysis of the DO and HI products. We thank Nancy Dowe, Thieny Trinh, and Andrew Lowell for initiating an earlier version of this study and for helpful discussions, and Eric Knoshaug for providing suggestions for several oleaginous yeast strains to examine. The views expressed in the article do not necessarily represent the views of the DOE or the U.S. Government. The U.S. Government retains and the publisher, by accepting the article for publication, acknowledges that the U.S. Government retains a nonexclusive, paid-up, irrevocable, worldwide license to publish or reproduce the published form of this work, or allow others to do so, for U.S. Government purposes.

References

1. A. Ragauskas, C. Williams, B. Davison, G. Britovsek, J. Cairney, C. Eckert, W. Frederick, J. Hallett, D. Leak, C. Liotta, J. Mielenz, R. Murphy, R. Templer and T. Tschaplinski, *Science*, 2006, **311**, 484 - 489.
2. L. R. Lynd, M. S. Laser, D. Bransby, B. E. Dale, B. Davison, R. Hamilton, M. Himmel, M. Keller, J. D. McMillan and J. Sheehan, *Nature Biotechnology*, 2008, **26**, 169-172.

3. G. Stephanopoulos, *Science*, 2007, **315**, 801-804.
4. J. N. Chheda, G. W. Huber and J. A. Dumesic, *Angewandte Chemie International Edition*, 2007, **46**, 7164-7183.
5. S. K. Lee, H. Chou, T. S. Ham, T. S. Lee and J. D. Keasling, *Current Opinion in Biotechnology*, 2008, **19**, 556-563.
6. H. Alper and G. Stephanopoulos, *Nature Reviews Microbiology*, 2009, **7**, 715-723.
7. M. R. Connor and J. C. Liao, *Current Opinion in Biotechnology*, 2009, **20**, 307-315.
8. J. C. Serrano-Ruiz and J. A. Dumesic, *Energy & Environmental Science*, 2011, **4**, 83-99.
9. S. Van de Vyver, J. Geboers, P. A. Jacobs and B. F. Sels, *ChemCatChem*, 2011, **3**, 82-94.
10. P. P. Peralta-Yahya, F. Zhang, S. B. del Cardayre and J. D. Keasling, *Nature*, 2012, **488**, 320-328.
11. J. C. Serrano-Ruiz, R. M. West and J. A. Dumesic, *Annual Review of Chemical and Biomolecular Engineering*, 2010, **1**, 79-100.
12. P. Mäki-Arvela, I. Kubickova, M. Snåre, K. Eränen and D. Y. Murzin, *Energy & Fuels*, 2007, **21**, 30-41.
13. M. K. Akhtar, N. J. Turner and P. R. Jones, *Proceedings of the National Academy of Sciences*, 2013, **110**, 87-92.
14. M. Snåre, I. Kubičková, P. Mäki-Arvela, K. Eränen and D. Y. Murzin, *Industrial & Engineering Chemistry Research*, 2006, **45**, 5708-5715.
15. E. J. Steen, Y. Kang, G. Bokinsky, Z. Hu, A. Schirmer, A. McClure, S. B. del Cardayre and J. D. Keasling, *Nature*, 2010, **463**, 559.
16. V. Sànchez Nogué and K. Karhumaa, *Biotechnology Letters*, 2015, **37**, 761-772.
17. J. Blazeck, A. Hill, L. Liu, R. Knight, J. Miller, A. Pan, P. Otoupal and H. S. Alper, *Nature Communications*, 2014, **5**.
18. M. Tai and G. Stephanopoulos, *Metabolic Engineering*, 2013, **15**, 1-9.
19. Y. A. Tsigie, C.-Y. Wang, C.-T. Truong and Y.-H. Ju, *Bioresource Technology*, 2011, **102**, 9216-9222.
20. K. Qiao, S. H. Imam Abidi, H. Liu, H. Zhang, S. Chakraborty, N. Watson, P. Kumaran Ajikumar and G. Stephanopoulos, *Metabolic Engineering*, 2015, **29**, 56-65.
21. M. Thiru, S. Sankh and V. Rangaswamy, *Bioresource Technology*, 2011, **102**, 10436-10440.
22. J. Zhang, X. Fang, X.-L. Zhu, Y. Li, H.-P. Xu, B.-F. Zhao, L. Chen and X.-D. Zhang, *Biomass and Bioenergy*, 2011, **35**, 1906-1911.
23. Y. Li, Z. K. Zhao and F. Bai, *Enzyme and Microbial Technology*, 2007, **41**, 312-317.
24. Z. Zhu, S. Zhang, H. Liu, H. Shen, X. Lin, F. Yang, Y. J. Zhou, G. Jin, M. Ye, H. Zou and Z. K. Zhao, *Nature Communications*, 2012, **3**, 1112.
25. C. Hu, X. Zhao, J. Zhao, S. Wu and Z. K. Zhao, *Bioresource Technology*, 2009, **100**, 4843-4847.
26. S. Wu, X. Zhao, H. Shen, Q. Wang and Z. K. Zhao, *Bioresource Technology*, 2011, **102**, 1803-1807.
27. J. Yaegashi, J. Kirby, M. Ito, J. Sun, T. Dutta, M. Mirsiaghi, E. R. Sundstrom, A. Rodriguez, E. Baidoo, D. Tanjore, T. Pray, K. Sale, S. Singh, J. D. Keasling, B. A. Simmons, S. W. Singer, J. K. Magnuson, A. P. Arkin, J. M. Skerker and J. M. Gladden, *Biotech. Biofuels*, 2017, **10**, 241.
28. C. Saenge, B. Cheirsilp, T. T. Suksaroge and T. Bourtoom, *Process Biochemistry*, 2011, **46**, 210-218.
29. E. R. Easterling, W. T. French, R. Hernandez and M. Licha, *Bioresource Technology*, 2009, **100**, 356-361.
30. G. Zhang, W. T. French, R. Hernandez, E. Alley and M. Paraschivescu, *Biomass and Bioenergy*, 2011, **35**, 734-740.
31. Z. Gong, Q. Wang, H. Shen, C. Hu, G. Jin and Z. K. Zhao, *Bioresource Technology*, 2012, **117**, 20-24.
32. C. Huang, X.-F. Chen, X.-Y. Yang, L. Xiong, X.-Q. Lin, J. Yang, B. Wang and X.-D. Chen, *Appl Biochem Biotechnol*, 2014, **172**, 2197-2204.
33. X. Zhao, X. Kong, Y. Hua, B. Feng and Z. K. Zhao, *European Journal of Lipid Science and Technology*, 2008, **110**, 405-412.
34. P. Xu, K. Qiao, W. S. Ahn and G. Stephanopoulos, *Proceedings of the National Academy of Sciences*, 2016, **113**, 10848-10853.
35. K. Qiao, T. M. Wasylenko, K. Zhou, P. Xu and G. Stephanopoulos, *Nature Biotechnology*, 2017, **35**, 173.
36. S. Zhang, M. Ito, J. M. Skerker, A. P. Arkin and C. V. Rao, *Applied Microbiology and Biotechnology*, 2016, **100**, 9393-9405.
37. M. S. Davis, J. Solbiati and J. E. Cronan, *Journal of Biological Chemistry*, 2000, **275**, 28593-28598.
38. X. Lu, H. Vora and C. Khosla, *Metabolic Engineering*, 2008, **10**, 333-339.
39. T. Liu, H. Vora and C. Khosla, *Metabolic Engineering*, 2010, **12**, 378-386.
40. J. Clomburg and R. Gonzalez, *Applied Microbiology and Biotechnology*, 2010, **86**, 419-434.
41. R. M. Lennen, D. J. Braden, R. M. West, J. A. Dumesic and B. F. Pfleger, *Biotechnology and Bioengineering*, 2010, **106**, 193-202.
42. P. Handke, S. A. Lynch and R. T. Gill, *Metabolic Engineering*, 2011, **13**, 28-37.
43. W. Runguphan and J. D. Keasling, *Metabolic Engineering*, 2014, **21**, 103-113.
44. N. A. Buijs, V. Siewers and J. Nielsen, *Current Opinion in Chemical Biology*, 2013, **17**, 480-488.
45. X. Tang, H. Feng and W. N. Chen, *Metabolic Engineering*, 2013, **16**, 95-102.
46. J. O. Valle-Rodríguez, S. Shi, V. Siewers and J. Nielsen, *Applied Energy*, 2014, **115**, 226-232.

47. I. R. Sitepu, L. A. Garay, R. Sestric, D. Levin, D. E. Block, J. B. German and K. L. Boundy-Mills, *Biotechnology Advances*, 2014, **32**, 1336-1360.
48. J. M. Ageitos, J. A. Vallejo, P. Veiga-Crespo and T. G. Villa, *Applied Microbiology and Biotechnology*, 2011, **90**, 1219-1227.
49. M. J. Biddy, R. Davis, D. Humbird, L. Tao, N. Dowe, M. T. Guarnieri, J. G. Linger, E. M. Karp, D. Salvachúa, D. R. Vardon and G. T. Beckham, *ACS Sustainable Chemistry & Engineering*, 2016, **4**, 3196-3211.
50. R. Davis, L. Tao, E. Tan, M. J. Biddy, G. T. Beckham, C. Scarlata, J. Jacobson, K. Cafferty, J. Ross, J. Lukas, D. Knorr and P. Schoen, *Process Design and Economics for the Conversion of Lignocellulosic Biomass to Hydrocarbons: Dilute-Acid Prehydrolysis and Enzymatic Hydrolysis Deconstruction of Biomass to Sugars and Biological Conversion of Sugars to Hydrocarbons*, NREL, Golden, CO, 2013.
51. P. J. Slininger, B. S. Dien, C. P. Kurtzman, B. R. Moser, E. L. Bakota, S. R. Thompson, P. J. O'Bryan, M. A. Cotta, V. Balan, M. Jin, L. d. C. Sousa and B. E. Dale, *Biotechnology and Bioengineering*, 2016, **113**, 1676-1690.
52. B. S. Dien, P. J. Slininger, C. P. Kurtzman, B. R. Moser and P. J. O'Bryan, *AIMS Environmental Science*, 2016, **3**, 1-20.
53. J. P. Sampaio, in *The Yeasts (Fifth Edition)*, eds. J. W. Fell and T. Boekhout, Elsevier, London, 2011, pp. 1873-1927.
54. J.-E. Lee, P. V. Vadlani and D. Min, *Journal of Sustainable Bioenergy Systems*, 2017, **7**, 36-50.
55. X. Yu, Y. Zheng, K. M. Dorgan and S. Chen, *Bioresource Technology*, 2011, **102**, 6134-6140.
56. Y.-H. Chang, K.-S. Chang, C.-L. Hsu, L.-T. Chuang, C.-Y. Chen, F.-Y. Huang and H.-D. Jang, *Fuel*, 2013, **105**, 711-717.
57. Y.-H. Chang, K.-S. Chang, C.-F. Lee, C.-L. Hsu, C.-W. Huang and H.-D. Jang, *Biomass and Bioenergy*, 2015, **72**, 95-103.
58. Q. Fei, M. O'Brien, R. Nelson, X. Chen, A. Lowell and N. Dowe, *Biotech. Biofuels*, 2016, **9**, 130.
59. X. Zhao, S. Wu, C. Hu, Q. Wang, Y. Hua and Z. K. Zhao, *Journal of Industrial Microbiology & Biotechnology*, 2010, **37**, 581-585.
60. J. Brandenburg, J. Blomqvist, J. Pickova, N. Bonturi, M. Sandgren and V. Passoth, *Yeast*, 2016, **33**, 451-462.
61. J. Wang, Q. Gao, H. Zhang and J. Bao, *Bioresource Technology*, 2016, **218**, 892-901.
62. X. Tang, H. Chen, Y. Q. Chen, W. Chen, V. Garre, Y. Song and C. Ratledge, *PLOS ONE*, 2015, **10**, e0128396.
63. D. Hardman, D. McFalls and S. Fakas, *Yeast*, 2017, **34**, 83-91.
64. S. Fakas, *Engineering in Life Sciences*, 2017, **17**, 292-302.
65. J. R. Petrie, T. Vanhercke, P. Shrestha, A. El Tahchy, A. White, X.-R. Zhou, Q. Liu, M. P. Mansour, P. D. Nichols and S. P. Singh, *PLOS ONE*, 2012, **7**, e35214.
66. G. M. Carman, *Biochemical Society Transactions*, 2005, **33**, 1150-1153.
67. R. Plaggenborg, J. Overhage, A. Loos, J. A. C. Archer, P. Lessard, A. J. Sinskey, A. Steinbüchel and H. Priefert, *Applied Microbiology and Biotechnology*, 2006, **72**, 745.
68. S. Mathew and T. E. Abraham, *Critical Reviews in Microbiology*, 2006, **32**, 115-125.
69. P. Wang, J. E. Brenchley and A. E. Humphrey, *Biotechnology Letters*, 1994, **16**, 977-982.
70. F. Koopman, N. Wierckx, J. H. de Winde and H. J. Ruijssenaars, *Proceedings of the National Academy of Sciences*, 2010, **107**, 4919-4924.
71. H. Ran, J. Zhang, Q. Gao, Z. Lin and J. Bao, *Biotech. Biofuels*, 2014, **7**, 51.
72. D. Feldman, D. J. Kowbel, N. L. Glass, O. Yarden and Y. Hadar, *Biotech. Biofuels*, 2015, **8**, 63.
73. C. Huang, H. Wu, T. J. Smith, Z. j. Liu, W. Y. Lou and M. h. Zong, *Biotechnology Letters*, 2012, **34**, 1637-1642.
74. I. Sárvári Horváth, C. J. Franzén, M. J. Taherzadeh, C. Niklasson and G. Lidén, *Applied and Environmental Microbiology*, 2003, **69**, 4076-4086.
75. N. Wierckx, F. Koopman, L. Bandounas, J. H. De Winde and H. J. Ruijssenaars, *Microbial Biotechnology*, 2010, **3**, 336-343.
76. M. T. Guarnieri, M. Ann Franden, C. W. Johnson and G. T. Beckham, *Metabolic Engineering Communications*, 2017, **4**, 22-28.
77. G. T. Beckham, C. W. Johnson, E. M. Karp, D. Salvachúa and D. R. Vardon, *Current Opinion in Biotechnology*, 2016, **42**, 40-53.
78. D. Salvachúa, E. M. Karp, C. T. Nimlos, D. R. Vardon and G. T. Beckham, *Green Chem.*, 2015, **17**, 4951-4967.
79. A. Yaguchi, A. Robinson, E. Mihealsick and M. Blenner, *Microbial Cell Factories*, 2017, **16**, 206.
80. J. P. Sampaio, *Canadian Journal of Microbiology*, 1999, **45**, 491-512.
81. S. A. Shields-Menard, M. AmirSadeghi, M. Green, E. Womack, D. L. Sparks, J. Blake, M. Edelmann, X. Ding, B. Sukhbaatar, R. Hernandez, J. R. Donaldson and T. French, *International Biodeterioration and Biodegradation*, 2017, **121**, 79-90.
82. D. R. Durham, C. G. McNamee and D. B. Stewart, *Journal of Bacteriology*, 1984, **160**, 771-777.
83. A. Gaal and H. Y. Neujahr, *Journal of Bacteriology*, 1979, **137**, 13-21.
84. S. Amara, N. Seghezzi, H. Otani, C. Diaz-Salazar, J. Liu and L. D. Eltis, *Scientific Reports*, 2016, **6**, 24985.

85. A. Rodriguez, D. Salvachúa, R. Katahira, B. A. Black, N. S. Cleveland, M. Reed, H. Smith, E. E. K. Baidoo, J. D. Keasling, B. A. Simmons, G. T. Beckham and J. M. Gladden, *ACS Sustainable Chemistry & Engineering*, 2017, **5**, 8171-8180.
86. R. K. Le, T. Wells Jr, P. Das, X. Meng, R. J. Stoklosa, A. Bhalla, D. B. Hodge, J. S. Yuan and A. J. Ragauskas, *RSC Advances*, 2017, **7**, 4108-4115.
87. Y. He, X. Li, H. Ben, X. Xue and B. Yang, *ACS Sustainable Chemistry & Engineering*, 2017, **5**, 2302-2311.
88. J. S. Kruger, N. S. Cleveland, R. Y. Yeap, T. Dong, K. J. Ramirez, N. J. Nagle, A. C. Lowell, G. T. Beckham, J. D. McMillan and M. J. Biddy, *ACS Sustainable Chemistry & Engineering*, 2018, DOI: 10.1021/acssuschemeng.7b01874.
89. L. M. L. Laurens, M. Quinn, S. Van Wychen, D. W. Templeton and E. J. Wolfrum, *Analytical and Bioanalytical Chemistry*, 2012, **403**, 167-178.
90. M. K. Conway, D. Grunwald and W. Heideman, *G3: Genes|Genomes|Genetics*, 2012, **2**, 1003-1017.
91. E. Van Donk, M. Lürling, D. O. Hessen and G. M. Lokhorst, *Limnology and Oceanography*, 1997, **42**, 357-364.
92. T. Dong, S. Van Wychen, N. Nagle, P. T. Pienkos and L. M. L. Laurens, *Algal Research*, 2016, **18**, 69-77.
93. H. G. Gerken, B. Donohoe and E. P. Knoshaug, *Planta*, 2013, **237**, 239-253.
94. M. Werner-Washburne, E. Braun, G. C. Johnston and R. A. Singer, *Microbiological Reviews*, 1993, **57**, 383-401.
95. Y.-K. Park, J.-M. Nicaud and R. Ledesma-Amaro, *Trends in Biotechnology*, 2017.
96. J. S. Kruger, E. D. Christensen, T. Dong, S. Van Wychen, G. M. Fioroni, P. T. Pienkos and R. L. McCormick, *Energy & Fuels*, 2017, **31**, 10946-10953.
97. M. Omidghane, E. Jenab, M. Chae and D. C. Bressler, *Energy & Fuels*, 2017, **31**, 9446-9454.
98. R. O. Idem, S. P. R. Katikaneni and N. N. Bakhshi, *Energy & Fuels*, 1996, **10**, 1150-1162.
99. H. J. Robota, J. C. Alger and L. Shafer, *Energy & Fuels*, 2013, **27**, 985-996.
100. J. Asomaning, P. Mussone and D. C. Bressler, *Journal of Analytical and Applied Pyrolysis*, 2014, **105**, 1-7.
101. D. McMillan James and T. Beckham Gregg, *Microbial Biotechnology*, 2016, **10**, 40-42.
102. F. Delvigne and H. Noorman, *Microbial Biotechnology*, 2017, **10**, 685-687.
103. D. Lamers, N. van Biezen, D. Martens, L. Peters, E. van de Zilver, N. Jacobs-van Dreumel, R. H. Wijffels and C. Lokman, *BMC Biotechnology*, 2016, **16**, 45.
104. R. Poontawee, W. Yongmanitchai and S. Limtong, *Process Biochemistry*, 2017, **53**, 44-60.
105. S. Fillet, J. Gibert, B. Suarez, A. Lara, C. Ronchel and J. L. Adrio, *Journal of Industrial Microbiolology & Biotechnology*, 2015, **42**, 1463-1472.
106. S. Shi and H. Zhao, *Frontiers in Microbiology*, 2017, **8**, 2185.
107. A. J. Martínez-Rodríguez and E. Pueyo, in *Wine chemistry and biochemistry*, eds. M. V. Moreno-Arribas and C. Polo, Springer-Verlag, New York, 2009, DOI: 10.1007/978-0-387-74118-5, ch. 3A, pp. 61-80.
108. V. Martínez, P. García, J. L. García and M. A. Prieto, *Microbial Biotechnology*, 2011, **4**, 533-547.
109. O. Pastinen, A. Nyyssölä, V. Pihlajaniemi and M. H. Sipponen, *Process Biochemistry*, 2017, **58**, 217-223.
110. B. E. Della-Bianca, T. O. Basso, B. U. Stambuk, L. C. Basso and A. K. Gombert, *Applied Microbiology and Biotechnology*, 2013, **97**, 979-991.
111. A. K. Gombert and A. J. A. van Maris, *Current Opinion in Biotechnology*, 2015, **33**, 81-86.
112. V. F. Tret'yakov, Y. I. Makarfi, K. V. Tret'yakov, N. A. Frantsuzova and R. M. Talyshinskii, *Catalysis in Industry*, 2010, **2**, 402-420.
113. N. Viswanadham, S. K. Saxena, J. Kumar, P. Sreenivasulu and D. Nandan, *Fuel*, 2012, **95**, 298-304.
114. J. J. Lovón-Quintana, J. K. Rodriguez-Guerrero and P. G. Valença, *Applied Catalysis A: General*, 2017, **542**, 136-145.
115. O. Muraza, *Industrial & Engineering Chemistry Research*, 2015, **54**, 781-789.
116. *US Pat.,* 20070287873A1, 2006.
117. *WO Pat.,* 2016160839A1, 2015.
118. E. Masai, Y. Katayama and M. Fukuda, *Bioscience, Biotechnology, and Biochemistry*, 2007, **71**, 1-15.
119. N. Kamimura, K. Katakahashi, K. Mori, T. Araki, M. Fujita, Y. Higuchi and E. Masa, *Environmental Microbiology Reports*, 2017, **9**, 679-705.